Table 5. Patient Background (Responders Versus Nonresponders)

	Responders (n=32)	Nonresponders (n=10)	OR (95% CI)*	P
Age, y	60.8±13.0	62.8±15.6	0.73 (0.30, 1.65)	0.59
Gender				
Male	27 (84.4)	7 (70.0)		0.56
Female	5 (15.6)	3 (30.0)	0.66 (0.25, 1.88)	
Diagnosis				
ASO	20 (62.5)	8 (80.0)		0.45
TAO	12 (37.5)	2 (20.0)	1.53 (0.61, 5.14)	
Ischemic status				
Fontaine 2	5 (15.6)	1 (10.0)		0.28
Fontaine 3	3 (9.4)	3 (30.0)	0.41 (0.07, 2.50)	
Fontaine 4	24 (75.0)	6 (60.0)	1.54 (0.32, 5.88)	
ABPI	0.77±0.30	0.75±0.39	0.87 (0.06, 12.3)	0.92
Rest pain scale	2.6±1.4	1.8±1.4	3.59 (0.74, 17.4)	0.18
Complications				
Diabetes	15 (46.9)	6 (60.0)	0.77 (0.32, 1.76)	0.71
Dyslipidemia	12 (37.5)	7 (70.0)	0.52 (0.19, 1.20)	0.15
Hypertension	18 (56.3)	7 (70.0)	0.75 (0.28, 1.74)	0.70
CRF on HD	13 (40.6)	6 (60.0)	0.68 (0.28, 1.55)	0.46
CAD	12 (37.5)	7 (70.0)	0.52 (0.19, 1.20)	0.15
CVD	12 (37.5)	2 (20.0)	1.53 (0.61, 5.14)	0.53
$CD34^+$ cells, $\times 10^7$	3.82±5.09	3.61±6.69	1.30 (0.70, 2.39)	0.49
Serum VEGF, pg/mL	187±112	119±27.9	5.70 (0.30, 108)	0.03

Data are shown as mean±SD or n (%). OR indicates odds ratio; CRF, chronic renal failure; HD, hemodialysis; CAD, coronary artery disease; CVD, cerebrovascular disease; VEGF, vascular endothelial growth factor.

*OR and 95% CI for OR.

factor and thus induced neovascularization of ischemic myocardium.

Discussion

In this study, we analyzed the long-term outcome of therapeutic neovascularization with PB-MNC. Overall, improvement of ischemic symptoms was observed in 60% to 70% of the treated patients. The annual major amputation rate was <10%, and the mortality rate was 20% at 2 years and 30% at 3 years in our patients (Figures 1G and 2A). In other populations similar to our patients, it has been reported that clinical improvement was achieved in 25% to 50% by standard therapy, whereas 30% to 50% of patients required major amputation within a year after conventional treatment.[20–23] The reported mortality rate for patients receiving standard treatment is ≈20% at 1 year and between 40% and 70% after 5 years.[20–23] Because this study was preliminary and did not have a placebo control group, it was difficult to assess precisely the efficacy and safety of cell therapy only in this study. Nevertheless, our results taken together with previous reports suggest that the performance of therapeutic neovascularization with PB-MNC might be safe and effective for patients with critical limb ischemia.

The improvement of rest pain and walking distance was less marked in ASO patients on dialysis (Figure 1D and 1E, Table 2, and supplemental Table II). Moreover, 4 of 5 major amputations occurred in ASO patients on dialysis (Figure 1G). Although it could be explained by an actual detrimental effect in ASO patients, it is possible that this treatment had been less effective for such patients. The survival rate of ASO patients on dialysis was lower than that of either nonhemodialysis ASO patients or TAO patients (Figure 2A), and most of the adverse events (death, major amputation, and cardiovascular events) occurred in the ASO group (mainly in patients on dialysis; Figures 1G and 2B). Thus, we need to be more cautious when we consider this treatment for ASO patients on dialysis. The worse outcome in these patients could be attributable to functional abnormalities of vascular cells and progenitor cells, which are associated with age and various risk factors.[24–26] For example, there is evidence of a decrease in the number and angiogenic activity of endothelial progenitor cells in patients with chronic renal failure,[27] and it was reported that such impairment was reversed by amelioration of uremia after renal replacement therapy.[28] In contrast, we found no significant difference in the number of progenitor cells between hemodialysis and nonhemodialysis patients (Table 3) or between responders and nonresponders (Table 5). We found that the number of progenitor cells was much lower in nonresponders from the nonhemodialysis group than in responders of the same group (supplemental Table VII), and similar findings were observed in the TAO group (supplemental Table V). However, no such differences were observed between responders and nonresponders in the hemodialysis group or the ASO group (supplemental Tables IV and VI), suggesting that the function of progenitor cells was impaired in nonresponders from these groups rather than cell numbers being reduced.

TAO patients showed a better response to this therapy than ASO patients with or without hemodialysis (supplemental Table II). None of the TAO patients died, and only 1 TAO patient underwent major amputation during the observation period, and few cardiovascular events occurred in this population (Figures 1G, 2A, and 2B), suggesting that TAO patients may be well suited for cell therapy. The better response of the TAO population may also have been achieved because they were younger and had fewer risk factors than ASO patients with or without hemodialysis.

The survival rate was very similar to the MACE-free rate, suggesting that cardiovascular disease influenced survival. Although cardiovascular events were not a direct cause of death in about half of the patients, they had several cardiovascular diseases (including stroke, coronary artery disease, and heart failure) that could compromise their ability to fight infection and regulate the fluid balance. Such impairment may in turn increase the incidence of severe infections like sepsis and aspiration pneumonia, as well as fatal renal failure. It has been suggested that neovascularization might induce the development of atherosclerotic plaque and that increased vascularity of atheroma could lead to plaque rupture.[29–31] Our previous study demonstrated that plasma levels of proangiogenic cytokines were increased after cell therapy, particularly in responders.[18] Therefore, we performed coronary angiogra-

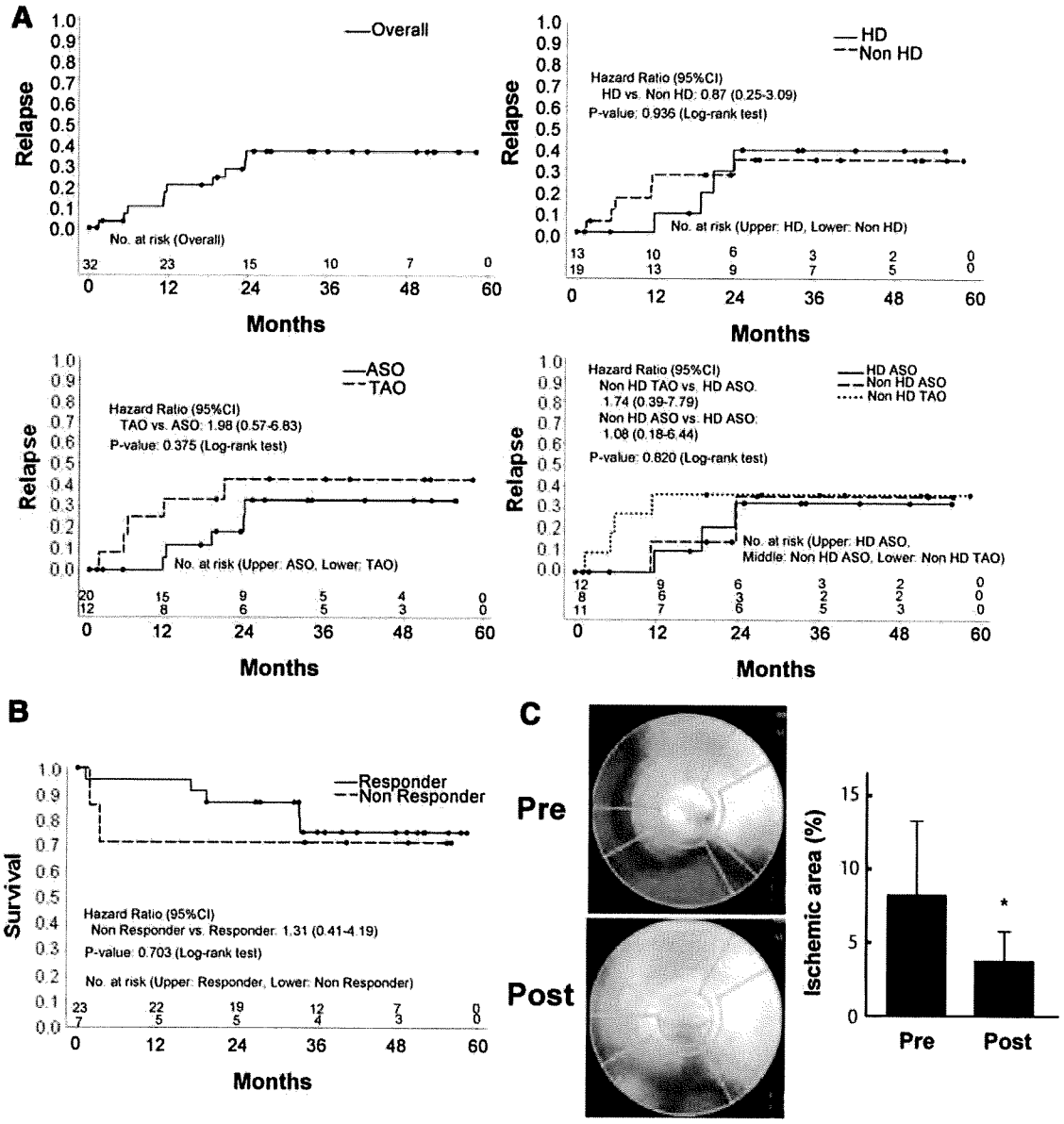

Figure 3. Relapse of ischemic symptoms. A, Relapse rates for ischemic symptoms. B, Survival rates of responders and nonresponders under 70 years old. C, Myocardial perfusion SPECT imaging of a responder with coronary artery disease before (Pre) and after (Post) treatment. *$P<0.05$ versus Pre.

phy and myocardial perfusion SPECT imaging in all of the patients both before and after treatment. There was no significant increase of cardiovascular events (including progression of coronary artery disease) in responders compared with nonresponders, suggesting that therapeutic neovascularization with PB-MNC did not promote atherogenesis. In fact, this therapy may have a beneficial rather than an adverse effect on coronary atherosclerosis because the area of myocardial ischemia estimated by SPECT imaging showed a significant decrease after treatment, and this improvement was associated with an increase in the plasma levels of proangiogenic factors. Moreover, survival tended to be better in responders younger than 70 years old. We previously demonstrated in a model of therapeutic neovascularization that implanted mononuclear cells could enhance muscle regeneration and increase the expression of various proangiogenic cytokines by regenerating myocytes, thus promoting vascularization and contributing to limb salvage. Taken together with our findings in animal studies, these clinical results suggest that this treatment increases the production of proangiogenic factors in ischemic limbs, thereby reducing myocardial ischemia as well as improving survival.

Limitations

This study was not placebo-controlled, and we did not analyze the data prospectively. The subjects were heterogeneous in terms of the underlying disease, age distribution, and coronary risk factors. Moreover, the survival rate of ASO patients was lower than that of TAO patients, although death was not directly related to limb ischemia. Therefore, it was difficult to assess precisely the efficacy of cell therapy in the present study.

Conclusion

Although this study was not placebo-controlled and we cannot assess the efficacy and safety of cell therapy only in this study, therapeutic angiogenesis with PB-MNC has a possibility of a safe and potentially effective treatment for critical limb ischemia. The results of a double-blind placebo-controlled study are needed to confirm our findings. Such a study is currently in progress.

Sources of Funding

This work was supported by a Grant-in-Aid for Scientific Research from the Ministry of Education, Science, Sports, and Culture; Health and Labor Sciences Research Grants (to I.K.); a Grant-in-Aid for Scientific Research from the Ministry of Education, Culture, Sports, Science, and Technology of Japan; and grants from the Suzuken Memorial Foundation, the Japan Diabetes Foundation, the Ichiro Kanehara Foundation, the Tokyo Biochemical Research Foundation, the Takeda Science Foundation, the Cell Science Research Foundation, and the Japan Foundation of Applied Enzymology (to T.M.).

Disclosures

None.

References

1. Braunwald E, Zipes DP, Libby P. *Heart Disease: A Textbook of Cardiovascular Medicine.* 6th ed. Philadelphia, Pa: WB Saunders; 2001.
2. Dormandy JA, Rutherford RB. Management of peripheral arterial disease (PAD). TASC Working Group. TransAtlantic Inter-Society Concensus (TASC). *J Vasc Surg.* 2000;31:S1–S296.
3. Carmeliet P. Mechanisms of angiogenesis and arteriogenesis. *Nat Med.* 2000;6:389–395.
4. Asahara T, Murohara T, Sullivan A, Silver M, van der Zee R, Li T, Witzenbichler B, Schatteman G, Isner JM. Isolation of putative progenitor endothelial cells for angiogenesis. *Science.* 1997;275:964–967.
5. Shi Q, Rafii S, Wu MH, Wijelath ES, Yu C, Ishida A, Fujita Y, Kothari S, Mohle R, Sauvage LR, Moore MA, Storb RF, Hammond WP. Evidence for circulating bone marrow-derived endothelial cells. *Blood.* 1998;92:362–367.
6. Asahara T, Masuda H, Takahashi T, Kalka C, Pastore C, Silver M, Kearne M, Magner M, Isner JM. Bone marrow origin of endothelial progenitor cells responsible for postnatal vasculogenesis in physiological and pathological neovascularization. *Circ Res.* 1999;85:221–228.
7. Rafii S, Lyden D. Therapeutic stem and progenitor cell transplantation for organ vascularization and regeneration. *Nat Med.* 2003;9:702–712.
8. Ikenaga S, Hamano K, Nishida M, Kobayashi T, Li TS, Kobayashi S, Matsuzaki M, Zempo N, Esato K. Autologous bone marrow implantation induced angiogenesis and improved deteriorated exercise capacity in a rat ischemic hindlimb model. *J Surg Res.* 2001;96:277–283.
9. Shintani S, Murohara T, Ikeda H, Ueno T, Sasaki K, Duan J, Imaizumi T. Augmentation of postnatal neovascularization with autologous bone marrow transplantation. *Circulation.* 2001;103:897–903.
10. Li TS, Hamano K, Suzuki K, Ito H, Zempo N, Matsuzaki M. Improved angiogenic potency by implantation of ex vivo hypoxia prestimulated bone marrow cells in rats. *Am J Physiol Heart.* 2002;283:H468–H473.
11. Tateishi-Yuyama E, Matsubara H, Murohara T, Ikeda U, Shintani S, Masaki H, Amano K, Kishimoto Y, Yoshimoto K, Akashi H, Shimada K, Iwasaka T, Imaizumi T. Therapeutic angiogenesis for patients with limb ischaemia by autologous transplantation of bone-marrow cells: A pilot study and a randomised controlled trial. *Lancet.* 2002;360:427–435.
12. Chen SL, Fang WW, Ye F, Liu YH, Qian J, Shan SJ, Zhang JJ, Chunhua RZ, Liao LM, Lin S, Sun JP. Effect on left ventricular function of intracoronary transplantation of autologous bone marrow mesenchymal stem cell in patients with acute myocardial infarction. *Am J Cardiol.* 2004;94:92–95.
13. Wollert KC, Meyer GP, Lotz J, Ringes-Lichtenberg S, Lippolt P, Breidenbach C, Fichtner S, Korte T, Hornig B, Messinger D, Arseniev L, Hertenstein B, Ganser A, Drexler H. Intracoronary autologous bone-marrow cell transfer after myocardial infarction: The BOOST randomised controlled clinical trial. *Lancet.* 2004;364:141–148.
14. Janssens S, Dubois C, Bogaert J, Theunissen K, Deroose C, Desmet W, Kalantzi M, Herbots L, Sinnaeve P, Dens J, Maertens J, Rademakers F, Dymarkowski S, Gheysens O, Van Cleemput J, Bormans G, Nuyts J, Belmans A, Mortelmans L, Boogaerts M, Van de Werf F. Autologous bone marrow-derived stem-cell transfer in patients with ST-segment elevation myocardial infarction: Double-blind, randomised controlled trial. *Lancet.* 2006;367:113–121.
15. Lunde K, Solheim S, Aakhus S, Arnesen H, Abdelnoor M, Egeland T, Endresen K, Ilebekk A, Mangschau A, Fjeld JG, Smith HJ, Taraldsrud E, Grogaard HK, Bjornerheim R, Brekke M, Muller C, Hopp E, Ragnarsson A, Brinchmann JE, Forfang K. Intracoronary injection of mononuclear bone marrow cells in acute myocardial infarction. *N Engl J Med.* 2006;355:1199–1209.
16. Schachinger V, Erbs S, Elsasser A, Haberbosch W, Hambrecht R, Holschermann H, Yu J, Corti R, Mathey DG, Hamm CW, Suselbeck T, Assmus B, Tonn T, Dimmeler S, Zeiher AM. Intracoronary bone marrow-derived progenitor cells in acute myocardial infarction. *N Engl J Med.* 2006;355:1210–1221.
17. Hristov M, Heussen N, Schober A, Weber C. Intracoronary infusion of autologous bone marrow cells and left ventricular function after acute myocardial infarction: A meta-analysis. *J Cell Mol Med.* 2006;10:727–733.
18. Tateno K, Minamino T, Toko H, Akazawa H, Shimizu N, Takeda S, Kunieda T, Miyauchi H, Oyama T, Matsuura K, Nishi J, Kobayashi Y, Nagai T, Kuwabara Y, Iwakura Y, Nomura F, Saito Y, Komuro I. Critical roles of muscle-secreted angiogenic factors in therapeutic neovascularization. *Circ Res.* 2006;98:1194–1202.
19. Minamino T, Toko H, Tateno K, Nagai T, Komuro I. Peripheral-blood or bone-marrow mononuclear cells for therapeutic angiogenesis? *Lancet.* 2002;360:2083–2084; author reply 2084.
20. Matsuno K, Kuwabara Y, Watanabe S, Kuroda T, Mikami Y, Fujii K, Saito T, Masuda Y. Detection of myocardial viability using rest-redistribution thallium-201 imaging in a stress 99Tcm-tetrofosmin/rest thallium-201 dual-isotope protocol. *Nucl Med Commun.* 2001;22:165–173.
21. Hirsch AT, Haskal ZJ, Hertzer NR, Bakal CW, Creager MA, Halperin JL, Hiratzka LF, Murphy WR, Olin JW, Puschett JB, Rosenfield KA, Sacks D, Stanley JC, Taylor LM Jr, White CJ, White J, White RA, Antman EM, Smith SC Jr, Adams CD, Anderson JL, Faxon DP, Fuster V, Gibbons RJ, Halperin JL, Hiratzka LF, Hunt SA, Jacobs AK, Nishimura R, Ornato JP, Page RL, Riegel B. ACC/AHA 2005 guidelines for the management of patients with peripheral arterial disease (lower extremity, renal, mesenteric, and abdominal aortic): executive summary a collaborative report from the American Association for Vascular Surgery/Society for Vascular Surgery, Society for Cardiovascular Angiography and Interventions, Society for Vascular Medicine and Biology, Society of Interventional Radiology, and the ACC/AHA Task Force on Practice Guidelines (Writing Committee to Develop Guidelines for the Management of Patients With Peripheral Arterial Disease) endorsed by the American Association of Cardiovascular and Pulmonary Rehabilitation; National Heart, Lung, and Blood Institute; Society for Vascular Nursing; TransAtlantic Inter-Society Consensus; and Vascular Disease Foundation. *J Am Coll Cardiol.* 2006;47:1239–1312.
22. Norgren L, Hiatt WR, Dormandy JA, Nehler MR, Harris KA, Fowkes FG. Inter-Society Consensus for the Management of Peripheral Arterial Disease (TASC II). *J Vasc Surg.* 2007;45(Suppl S):S5–S67.
23. Weitz JI, Byrne J, Clagett GP, Farkouh ME, Porter JM, Sackett DL, Strandness DE Jr, Taylor LM. Diagnosis and treatment of chronic arterial insufficiency of the lower extremities: A critical review. *Circulation.* 1996;94:3026–3049.
24. Brass EP, Anthony R, Dormandy J, Hiatt WR, Jiao J, Nakanishi A, McNamara T, Nehler M. Parenteral therapy with lipo-ecraprost, a lipid-based formulation of a PGE1 analog, does not alter six-month outcomes in patients with critical leg ischemia. *J Vasc Surg.* 2006;43:752–759.
25. Ballard VL, Edelberg JM. Stem cells and the regeneration of the aging cardiovascular system. *Circ Res.* 2007;100:1116–1127.
26. Hill JM, Zalos G, Halcox JP, Schenke WH, Waclawiw MA, Quyyumi AA, Finkel T. Circulating endothelial progenitor cells, vascular function, and cardiovascular risk. *N Engl J Med.* 2003;348:593–600.
27. Reed MJ, Edelberg JM. Impaired angiogenesis in the aged. *Sci Aging Knowledge Environ.* 2004;2004:pe7.
28. Choi JH, Kim KL, Huh W, Kim B, Byun J, Suh W, Sung J, Jeon ES, Oh HY, Kim DK. Decreased number and impaired angiogenic function of endothelial progenitor cells in patients with chronic renal failure. *Arterioscler Thromb Vasc Biol.* 2004;24:1246–1252.

29. de Groot K, Bahlmann FH, Sowa J, Koenig J, Menne J, Haller H, Fliser D. Uremia causes endothelial progenitor cell deficiency. *Kidney Int.* 2004;66:641–646.
30. Moulton KS, Heller E, Konerding MA, Flynn E, Palinski W, Folkman J. Angiogenesis inhibitors endostatin or TNP-470 reduce intimal neovascularization and plaque growth in apolipoprotein E-deficient mice. *Circulation.* 1999;99:1726–1732.
31. Celletti FL, Waugh JM, Amabile PG, Brendolan A, Hilfiker PR, Dake MD. Vascular endothelial growth factor enhances atherosclerotic plaque progression. *Nat Med.* 2001;7:425–429.

CLINICAL PERSPECTIVE

Injection of bone marrow mononuclear cells has been reported to promote neovascularization of ischemic tissues effectively. We found that peripheral blood mononuclear cells were as efficient as bone marrow mononuclear cells for the treatment of limb ischemia in animals, and we showed that this treatment was feasible in no-option patients with limb ischemia. However, the long-term outcome of such therapy has not been investigated. In this study, we assessed the long-term outcome of patients receiving this treatment. Improvement of ischemic symptoms was observed in 60% to 70% of the patients. The annual rate of major amputation was decreased markedly by treatment. Improvement of ischemic symptoms was less marked in arteriosclerosis obliterans (ASO) patients on dialysis compared with nonhemodialysis ASO or thromboangiitis obliterans patients. Indeed, the survival rate of these patients was lower than that of nonhemodialysis ASO or thromboangiitis obliterans patients. Major adverse events such as death, major amputation, and cardiovascular events occurred mostly in ASO patients, and most of them were on dialysis. Thus, we need to be more cautious when we consider this treatment for ASO patients on dialysis. Although it has been suggested that neovascularization might induce the development of atherosclerotic plaque, there was no significant increase of cardiovascular events in responders compared with nonresponders in our study, suggesting that therapeutic neovascularization with peripheral blood mononuclear cells did not promote atherogenesis. Collectively, injection of peripheral blood mononuclear cells seems safe and potentially effective for the treatment of limb ischemia, but the results of a double-blind placebo-controlled study are needed to confirm our findings.

Protective Role of SIRT1 in Diabetic Vascular Dysfunction

Masayuki Orimo, Tohru Minamino, Hideyuki Miyauchi, Kaoru Tateno, Sho Okada, Junji Moriya, Issei Komuro

Objective—Calorie restriction (CR) prolongs the lifespan of various species, ranging from yeasts to mice. In yeast, CR extends the lifespan by increasing the activity of silencing information regulator 2 (Sir2), an NAD^+-dependent deacetylase. SIRT1, a mammalian homolog of Sir2, has been reported to downregulate p53 activity and thereby prolong the lifespan of cells. Although recent evidence suggests a link between SIRT1 activity and metabolic homeostasis during CR, its pathological role in human disease is not yet fully understood.

Methods and Results—Treatment of human endothelial cells with high glucose decreases SIRT1 expression and thus activates p53 by increasing its acetylation. This in turn accelerates endothelial senescence and induces functional abnormalities. Introduction of SIRT1 or disruption of p53 inhibits high glucose–induced endothelial senescence and dysfunction. Likewise, activation of Sirt1 prevents the hyperglycemia-induced vascular cell senescence and thereby protects against vascular dysfunction in mice with diabetes.

Conclusions—These findings represent a novel mechanism of vascular cell senescence induced by hyperglycemia and suggest a protective role of SIRT1 in the pathogenesis of diabetic vasculopathy. **(*Arterioscler Thromb Vasc Biol.* 2009; 29:889-894.)**

Key Words: cellular senescence ■ p53 ■ diabetes

The NAD^+-dependent histone deacetylase Sir2 induces longevity in yeast in response to calorie restriction signals.[1] SIRT1, a mammalian homologue of Sir2 and a member of the Sir2 family called sirtuins, has been shown to target p53,[2–4] Ku70,[5] and the forkhead transcription factors[6–8] for deacetylation, thereby regulating stress responses, apoptosis, and cellular senescence. Acetylation of p53 is known to be crucial for its stabilization and transcriptional activation.[9] Accumulating evidence suggests that SIRT1 also modulates the metabolism of glucose and fat by interacting with peroxisome proliferator-activated receptor (PPAR) γ through nuclear receptor corepressor to repress adipogenesis,[10] modifying PPAR γ coactivator-1α to regulate hepatic glucose homeostasis[11,12] and regulating insulin secretion levels as well as insulin sensitivity.[13–15] Treatment with the sirtuin activator resveratrol has been shown to improve diet-induced obesity and insulin resistance[16,17] and delay age-related deterioration including increased arterial stiffness.[18] Moreover, Sirt1 has been reported to control endothelial angiogenic functions during postnatal vascular growth.[19] However, it remains unclear whether SIRT1 is involved in the pathogenesis of diabetes and its complications including diabetic vasculopathy.

Vascular cells have a finite lifespan when cultured and eventually undergo senescence. Many of the changes seen in senescent vascular cells are consistent with those that occur in age-related vascular diseases.[20,21] Moreover, senescent vascular cells have been detected in human atherosclerotic tissues and exhibit various functional abnormalities,[22] suggesting that senescence of vascular cells contributes to the pathophysiology of age-related vascular diseases. There is also in vivo evidence for the occurrence of vascular cell senescence in diabetic vasculopathy.[23] Given that CR augments SIRT1 activity, hyperglycemia might induce vascular cell senescence by reducing SIRT1 activity and thereby contribute to the development of diabetic vasculopathy. In the present study we show a novel mechanism of vascular cell senescence induced by hyperglycemia. Hyperglycemia decreases SIRT1 expression and thus activates p53 by increasing its acetylation. Activation of SIRT1 prevents the hyperglycemia-induced vascular cell senescence and thereby protects against vascular dysfunction in mice with diabetes. These results suggest a protective role of SIRT1 in the pathogenesis of diabetic vasculopathy.

Materials and Methods

Cell Culture

Human umbilical vein endothelial cells were purchased from Bio Whittaker (Walkersville, Md) and cultured according to the manufacturer's instructions. We defined senescent cells as the cultures that do not increase for 2 weeks at subcofluent and confirmed with

Received February 3, 2009; revision accepted March 3, 2009.

From the Department of Cardiovascular Science and Medicine, Chiba University Graduate School of Medicine, Japan.
M.O. and T.M. contributed equally to this study.
Correspondence to Issei Komuro, MD, PhD, Department of Cardiovascular Science and Medicine, Chiba University Graduate School of Medicine, 1-8-1 Inohana, Chuo-ku, Chiba 260-8670, Japan. E-mail komuro-tky@umin.ac.jp

Arterioscler Thromb Vasc Biol **is available at http://atvb.ahajournals.org** **DOI: 10.1161/ATVBAHA.109.185694**

senescence-associated β-galactosidase activity assay. Senescence-associated β-galactosidase staining was performed as described.[22]

Retroviral Infection

pBabe (a gift from Dr C.W. Lowe, Cold Spring Harbor Laboratory, Cold Spring Harbor, NY) was used for generating retroviruses. pBabe SIRT1 was a kind gift from Dr T. Kouzarides, Wellcome Institute, Cambridge, UK. We constructed the pBabe-based vector expressing E6 (pBabe E6). Details of the construct are available on request. Retroviral stocks were generated by transient transfection of packaging cell line and stored at −80°C until use. Human endothelial cells (passage 4 to 6) were plated at 5×10^5 cells per 100-mm-diameter dish 24 hours before infections. For infections, the culture medium was replaced by retroviral stocks supplemented with 8 μg/mL polybrene (Sigma). Forty-eight hours after infections, the infected cell populations were selected by culture in 0.8 μg/mL puromycin for 4 days (pBabe-based vectors). After selection, 1 to 3×10^5 cells were seeded onto 100-mm-diameter dish.

Western Blot Analysis and Antibodies

Whole-cell lysates (30 μg) were resolved by SDS polyacrylamide gel electrophoresis (PAGE). Proteins were transferred onto a polyvinylidene difluoride membrane (Millipore) and incubated with the first antibody followed by an anti-rabbit immunoglobulin G-horseradish peroxidase antibody or anti-mouse immunoglobulin G-horseradish peroxidase antibody (Jackson). Specific proteins were detected using enhanced chemiluminescence (Amersham). The first antibodies used for Western blotting are as follows: antibodies to p53, ICAM-1, actin, and tubulin (Santa Cruz); antip21 antibody (Oncogene); antiacetylated p53 antibody (Cell Signaling); anti-SIRT1 antibody (Upstate Biotechnology).

Northern Blot Analysis

Total RNA (30 μg) was extracted using RNA zol B (Tel Test) according to the manufacturer's instructions, separated on a formaldehyde denaturing gel and transferred to a nylon membrane (Amersham). The blot was then hybridized with radiolabeled cDNA probes for *p21* using the Quickhyb hybridization solution (Stratagene) according to the manufacturer's instructions.

Luciferase Assay

The reporter gene plasmid (1 μg) was transfected into endothelial cells in medium containing various glucose concentrations. In some experiments, cells were infected with retroviral vectors 24 hours before luciferase assay. The control vector encoding *Renilla* luciferase (0.1 μg) was cotransfected for an internal control. Luciferase assay was carried out using dual-luciferase reporter assay system (Promega) according to the manufacturer's instructions. The plasmid pPG13-Luc containing the p53-binding sequence was a gift from Dr B. Vogelstein (Johns Hopkins University, Baltimore, Md).

Histology

For immunohistochemistry, the frozen sections (6 μm) were treated with 0.3% hydrogen peroxide in methanol for 20 minutes, preincubated with 5% goat serum and then treated with anti-Sirt antibody (Upstate Biotechnology), anti-p53 antibody, or anti–ICAM-1 antibody (Santa Cruz) overnight at 4°C. Next, the sections were incubated with a biotinylated goat secondary antibody, treated with the avidin-biotin complex (Elite ABC kit, Vector) and stained with diaminobenzidine tetrahydrochloride and hydrogen peroxide. Senescence-associated β galactosidase activity assay was performed as described previously.[22]

Statistical Analysis

Data were shown as mean±SEM. Multiple group comparison was performed by 1-way ANOVA followed by the Bonferroni procedure for comparison of means. Comparisons between 2 groups were analyzed by 2-way ANOVA. Values of $P<0.05$ were considered statistically significant.

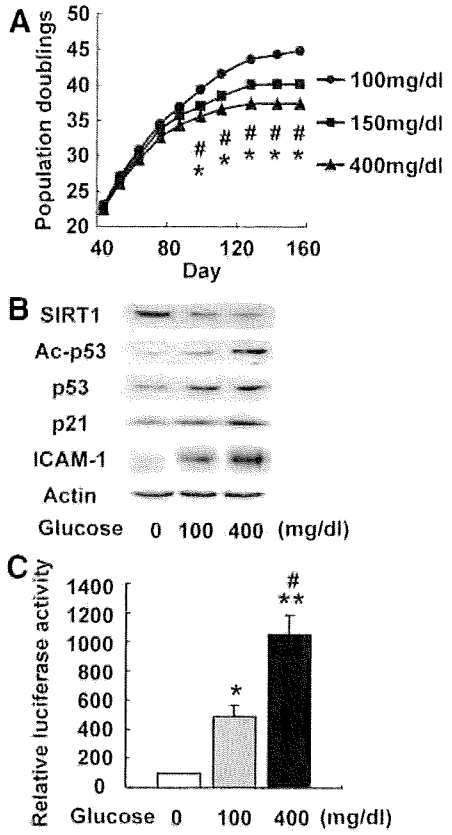

Figure 1. High glucose–induced endothelial cell senescence. A, Human endothelial cells were passaged in medium containing various concentrations of glucose, and cell lifespan was determined. *$P<0.05$ vs 100 mg/dL glucose; #$P<0.05$ vs 150 mg/dL glucose. n=3. B, Human endothelial cells were cultured in medium containing various concentrations of glucose for 24 hours and harvested to examine SIRT1, acetylated p53 (Ac-p53), p53, p21, and ICAM-1 levels by Western blot analysis. C, Transcriptional activity of p53 was examined by luciferase assay in endothelial cells exposed to glucose at the indicated concentration. *$P<0.05$, **$P<0.01$ vs 0 mg/dL glucose; #$P<0.05$ vs 100 mg/dL glucose. Error bars indicate SEM; n=4.

Results

Treatment With High Glucose Accelerates Endothelial Cell Senescence

To examine the effects of high glucose on the lifespan of vascular cells, human vascular endothelial cells were passaged in medium containing various concentrations of glucose (100, 150, and 400 mg/dL) until senescence occurred. The osmotic pressure of each medium was adjusted to that of the high-glucose (400 mg/dL) medium by the addition of mannitol. Exposure to a very high concentration of glucose (400 mg/dL) decreased the lifespan of human endothelial cells, and the effects of glucose were dose-dependent (Figure 1A). SIRT1 expression was decreased and acetylated p53 was increased in human endothelial cells by culture in high-glucose medium (Figure 1B and supplemental Figure I, available online at http://atvb.ahajournals.org). Consistent with these results, culture in high-glucose medium increased transcriptional activity of p53 (Figure 1C) and thereby upregulated expression of the cyclin-dependent kinase inhibitor $p21^{Waf1/Cip1}$ (Figure 1B and supplemental Figure I). Culture

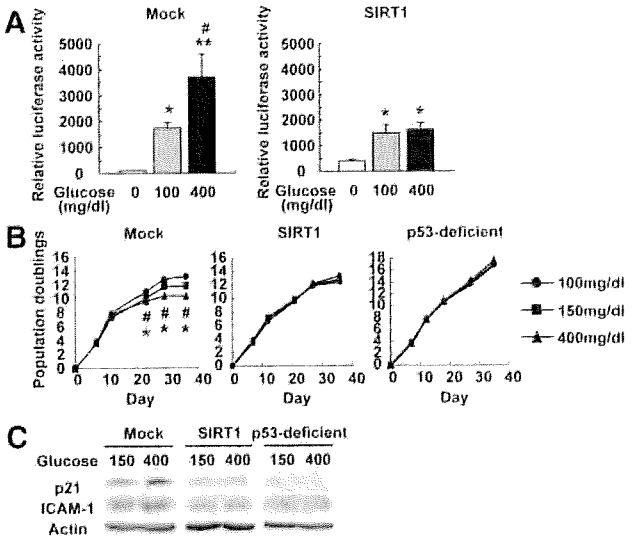

Figure 2. Critical roles of SIRT1 and p53 activity in high glucose-induced senescence. A, Endothelial cells were infected with pBabe (Mock) or pBabe SIRT1 (SIRT1) and exposed to medium containing various concentrations of glucose, after which transcriptional activity of p53 was examined by luciferase assay. *$P<0.05$, **$P<0.01$ vs 0 mg/dL glucose; #$P<0.05$ vs 100 mg/dL glucose. n=3. B, Human endothelial cells were infected with pBabe, pBabe SIRT1, or pBabe E6 (the oncoprotein of HPV16 that ablates p53), and cell lifespan was determined. *$P<0.05$ vs 100 mg/dL glucose; #$P<0.05$ vs 150 mg/dL glucose. n=3. C, Western blot analysis for the expression of p21 and ICAM-1 in endothelial cells prepared in B.

in high-glucose medium also upregulated the expression of intracellular adhesion molecule-1 (ICAM-1), a crucial receptor that mediates cell-cell interactions and plays a critical role in the development of atherosclerosis (Figure 1B and supplemental Figure I).

SIRT1 Inhibits High Glucose-Induced Endothelial Cell Senescence

To investigate whether SIRT1 was involved in high glucose–induced senescence, we examined the effect of increased SIRT1 expression on activation of p53 by high glucose. Exposure to high-glucose medium increased p53 activity in mock-infected cells (Figure 2A), although this increase was significantly inhibited by introduction of SIRT1, suggesting that induction of p53 by high glucose was related to a decrease of SIRT1 expression (Figure 2A). We next examined the relationship between SIRT1 and the reduction of cellular lifespan by high-glucose conditions. We infected human endothelial cells with a retroviral vector encoding SIRT1 or an empty vector (mock), and then cultured the cells with various concentrations of glucose until senescence occurred. We also examined the effect of ablation of p53. Exposure to high glucose medium shortened the lifespan of mock-infected cells, whereas this effect of glucose was prevented by constitutive expression of SIRT1 (Figure 2B). In addition, the ablation of p53 activity prevented the acceleration of cellular aging by culture under high-glucose conditions (Figure 2B). Consistent with the previous report,[24] treatment with sirtinol, a specific inhibitor for sirtuins, promoted cellular senescence under normal-glucose conditions

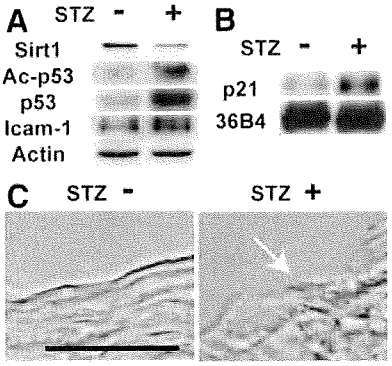

Figure 3. Hyperglycemia induces endothelial senescence in vivo. A, Mice were given vehicle (−) or streptozotocin (STZ; +). The aortas were harvested 4 weeks after administration and examined for Sirt1, acetylated p53 (Ac-p53), p53, and ICAM-1 levels by Western blot analysis. B, The aortas prepared in A were examined for *p21* expression by Northern blot analysis. C, The aortas prepared in A were subjected to senescence-associated β galactosidase activity assay. Arrow indicates positive (senescent) endothelial cells. Scale bar=5 μm.

(data not shown). These results indicated that downregulation of SIRT1 expression was responsible for high glucose–induced senescence. Moreover, the induction of ICAM-1 and p21 expression by exposure to high-glucose medium was inhibited by either introduction of SIRT1 or ablation of p53 activity (Figure 2C), suggesting a potential role of the SIRT1/p53 axis in diabetic vasculopathy.

Decreased Expression of Sirt1 Is Associated With Vascular Senescence in Diabetic Mice

To further investigate whether Sirt1 is involved in the pathogenesis of diabetic vasculopathy, we produced a mouse model of diabetes by treatment with streptozotocin and harvested the aorta after 4 weeks. Western blot analysis revealed that expression level of Sirt1was significantly lower in the aortas of diabetic mice than in those of nondiabetic mice (Figure 3A and supplemental Figure IIA). Consistent with this finding, levels of acetylated p53 and p21 expression were significantly higher in the aortas of diabetic mice compared with those of control mice (Figure 3A and 3B and supplemental Figure IIA). Histological analyses revealed that an increase of senescence-associated β galactosidase activity (a biomarker for cellular senescence) was predominantly observed in aortic endothelial cells of diabetic mice and that this increase was associated with downregulation of Sirt1 expression and upregulation of p53 expression in aortic endothelial cells (Figure 3C and supplemental Figure IIB). These results suggest that hyperglycemia induced p53-dependent endothelial cell senescence. Furthermore, the expression of ICAM-1 was significantly increased in aortic endothelial cells of diabetic mice (Figure 3A and supplemental Figure IIA and IIB). We thus speculated that activation of Sirt1 might improve vascular dysfunction in diabetic mice.

Resveratrol Improves Vascular Dysfunction in Diabetic Mice

To test our hypothesis, we treated diabetic mice with resveratrol, a sirtuin activator.[25,26] Injection of streptozotocin markedly decreased the plasma insulin below detectable levels and

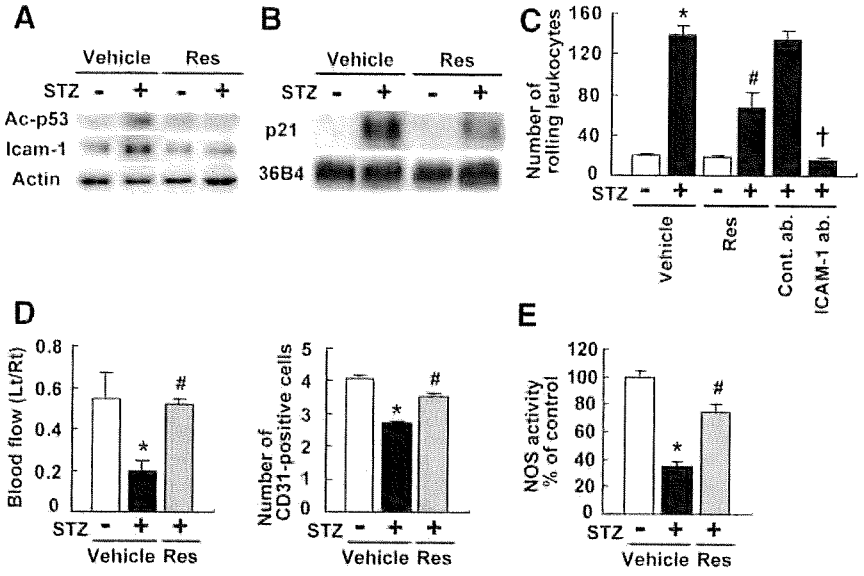

Figure 4. Critical roles of SIRT1 and p53 activity in diabetic vasculopathy. A through C, Mice were given vehicle (−) or streptozotocin (+) and treated with resveratrol (Res) or vehicle. Acetylated p53 (Ac-p53), Icam-1 (A), and *p21* expression (B) in the aorta. C, The number of rolling leukocytes (C). *$P<0.05$ vs STZ (−)/Vehicle; #$P<0.05$ vs STZ (+)/Vehicle; †$P<0.01$ vs STZ (+)/Control antibody. n=3. D, A hind limb ischemia model was generated in mice prepared in A. *$P<0.01$ vs STZ (−)/Vehicle; #$P<0.01$ vs STZ (+)/Vehicle. n=4. E, Nitric oxide synthase (NOS) activity in the aorta was measured in mice prepared in A. *$P<0.01$ vs STZ (−)/Vehicle; #$P<0.01$ vs STZ (+)/Vehicle. n=4.

the plasma glucose level gradually increased (supplemental Figure IIIA). Resveratrol did not affect the increase of plasma glucose after streptozotocin treatment (supplemental Figure IIIA). Indeed, there were no differences of plasma insulin, cholesterol, or triglyceride levels between vehicle-treated and reveratrol-treated diabetic mice (supplemental Figure IIIA and data not shown). Thus, resveratrol did not seem to improve the diabetic state in this experimental setting. However, resveratrol reduced the acetylated p53 level and suppressed induction of p21 expression in the aortas of diabetic mice (Figure 4A and 4B and supplemental Figure IIIB and IIIC), suggesting that activation of sirtuins prevented vascular cell senescence accelerated by hyperglycemia. An increase of leukocyte rolling and adhesion is known to be an initial step in the development of atherosclerosis, and ICAM-1 is thought to be a key endothelial receptor involved in these events. Therefore, we examined the effects of resveratrol on ICAM-1 expression in the aortas of diabetic mice. We found that the expression of ICAM-1 was significantly lower in resveratrol-treated diabetic mice compared with vehicle-treated mice (Figure 4A and supplemental Figure IIIB). Next, we investigated whether resveratrol reduced leukocyte rolling and adhesion in diabetic mice. Using an intravital microscopy, we observed that hyperglycemia significantly promoted leukocyte rolling and adhesion in the femoral artery, whereas these changes were markedly inhibited by treatment with resveratrol as well as by administration of anti–ICAM-1 neutralizing antibody (Figure 4C and supplemental movies), indicating that resveratrol treatment downregulates ICAM-1 expression, thereby inhibiting leukocyte rolling and adhesion. In contrast, resveratrol had little influence on aortic ICAM-1 expression or leukocyte rolling in p53-deficient mice (data not shown), suggesting that resveratrol inhibited p53-dependent vascular cell senescence induced by hyperglycemia and thereby protected diabetic mice against vascular dysfunction. Protective roles of Sirt1 in diabetic vasculopathy were further supported by the observations that resveratrol treatment significantly increased neovascularization in ischemic limbs and nitric oxide synthase activity in diabetic mice (Figure 4D and 4E). Thus, activation of Sirt1 may be a novel strategy for the treatment of diabetic vascular complications.

The Akt/FOXO Pathway Plays a Crucial Role in the Downregulation of SIRT1 Expression by High-Glucose Conditions

The forkhead box O transcription factor (FOXO) has been shown to positively regulate SIRT1 expression.[27] Because hyperglycemia has been reported to increase Akt activity,[28,29] we investigated whether these signaling molecules were involved in the regulation of SIRT1 expression under high-glucose conditions. Exposure of human endothelial cells to a high concentration of glucose led to an increase of phospho-Akt (supplemental Figure IVA). When this pathway was disrupted by introducing a dominant-negative form of Akt, exposure of cells to high glucose failed to affect the levels of SIRT1 and acetylated p53 (supplemental Figure IVB), suggesting a critical role of the Akt signaling pathway in the downregulation of SIRT1 expression by high-glucose conditions.

Discussion

In the present study, we demonstrated a novel mechanism of diabetic vasculopathy. Hyperglycemia reduces Sirt1 expression, leading to p53-dependent vascular cell senescence and thus to vascular dysfunction. It remains unclear how hyperglycemia downregulates Sirt1 expression. FOXO has been shown to positively regulate SIRT1 expression.[27] Akt phosphorylates FOXO and thus blocks its transcriptional activity by promoting cytoplasmic retention and degradation, and it has been reported that hyperglycemia upregulates Akt activity.[28,29] The AMP-activated protein kinase (AMPK) plays a critical role in the cellular responses to low energy levels, and phosphorylation by AMPK leads to the activation of FOXO transcriptional activity without affecting FOXO subcellular localization.[30] Because phospho-Akt levels were increased and phospho-AMPK levels were reduced in the aortas of diabetic mice compared with those of nondiabetic mice (M. Orimo, T. Minamino, unpublished data, 2008), hyperglycemia may downregulate expression of Sirt1 by decreasing FOXO

activity. Consistent with this idea, our in vitro experiments showed that treatment of human endothelial cells with high glucose led to activation of Akt and a decrease of SIRT1 expression. This decrease was significantly inhibited by introduction of a dominant-negative form of Akt, suggesting that the downregulation of SIRT1 expression by high-glucose conditions is at least partially mediated by the Akt/FOXO signaling pathway.

SIRT1-mediated deacetylation of p53 prevents p53-dependent transactivation of various target genes such as p21 and Bax. These direct effects of SIRT1 on p53 transactivation are important for the function of p53 as a transcription factor because the acetylation status has been shown to be indispensable for its ability to repress cell growth and induce apoptosis.[31] It has been reported that the inhibition of cellular deacetylases leads to a longer half-life for endogenous p53, indicating that acetylation of p53 also contributes to p53 stabilization.[32] Thus, SIRT1 may negatively regulate the ability of p53 to promote endothelial senescence by inhibiting its transcriptional activity as well as by inducing its degradation. In addition to being a direct effector of SIRT1 deacetylation, p53 can repress *SIRT1* transcription by binding to 2 response elements within the *SIRT1* promoter,[27] which suggests that SIRT1 and p53 exist in a negative-regulatory feedback loop: hyperglycemia-induced downregulation of SIRT1 may further decrease its expression via p53 activation.

We have previously reported that activation of the insulin/Akt pathway enhances the aging of cultured human endothelial cells via the p53/p21-dependent pathway.[33] This effect is partly mediated by a decrease of FOXO activity, which leads to downregulation of antioxidant genes and an increase of the intracellular level of reactive oxygen species (ROS).[33] Therefore, both hyperinsulinemia and hyperglycemia may induce vascular cell senescence through mechanisms involving SIRT1-dependent and -independent pathways, thereby promoting vascular complications in patients with type 2 diabetes. An increase of oxidative stress is associated with most of the pathways that have been implicated in diabetic vasculopathy including the polyol pathway and the protein kinase C pathway.[34] Thus, these pathways may also promote p53-dependent vascular cell senescence by increasing ROS levels.

In addition to p21 expression, ICAM-1 was induced by hyperglycemia, and its induction was disrupted by ablation of p53. This finding was in accordance with a previous report that p53 directly activates ICAM-1 expression in an NF-κB–independent manner.[35] Senescent cells also exhibit various features of endothelial dysfunction such as decreased production of nitric oxide and increased expression of cytokines and coagulators.[20] Thus, inhibition of vascular cell senescence by activation of SIRT1 may be a potential therapeutic strategy for human vascular diseases.

Sources of Funding

This work was supported by a Grant-in-Aid for Scientific Research from the Ministry of Education, Science, Sports, and Culture, and Health and Labor Sciences Research Grants, and a Research Grant from the Mitsubishi Foundation (to I.K.) and a Grant-in-Aid for Scientific Research from the Ministry of Education, Culture, Sports, Science, and Technology of Japan, and the grants from the Suzuken Memorial Foundation, the Japan Diabetes Foundation, the Ichiro Kanehara Foundation, the Tokyo Biochemical Research Foundation, the Takeda Science Foundation, the Cell Science Research Foundation, and the Japan Foundation of Applied Enzymology (to T.M.).

Disclosures

None.

References

1. Lin SJ, Kaeberlein M, Andalis AA, Sturtz LA, Defossez PA, Culotta VC, Fink GR, Guarente L. Calorie restriction extends Saccharomyces cerevisiae lifespan by increasing respiration. *Nature*. 2002;418:344–348.
2. Luo J, Nikolaev AY, Imai S, Chen D, Su F, Shiloh A, Guarente L, Gu W. Negative control of p53 by Sir2alpha promotes cell survival under stress. *Cell*. 2001;107:137–148.
3. Vaziri H, Dessain SK, Ng Eaton E, Imai SI, Frye RA, Pandita TK, Guarente L, Weinberg RA. hSIR2(SIRT1) functions as an NAD-dependent p53 deacetylase. *Cell*. 2001;107:149–159.
4. Langley E, Pearson M, Faretta M, Bauer UM, Frye RA, Minucci S, Pelicci PG, Kouzarides T. Human SIR2 deacetylates p53 and antagonizes PML/p53-induced cellular senescence. *Embo J*. 2002;21:2383–2396.
5. Cohen HY, Miller C, Bitterman KJ, Wall NR, Hekking B, Kessler B, Howitz KT, Gorospe M, de Cabo R, Sinclair DA. Calorie restriction promotes mammalian cell survival by inducing the SIRT1 deacetylase. *Science*. 2004;305:390–392.
6. Motta MC, Divecha N, Lemieux M, Kamel C, Chen D, Gu W, Bultsma Y, McBurney M, Guarente L. Mammalian SIRT1 represses forkhead transcription factors. *Cell*. 2004;116:551–563.
7. Brunet A, Sweeney LB, Sturgill JF, Chua KF, Greer PL, Lin Y, Tran H, Ross SE, Mostoslavsky R, Cohen HY, Hu LS, Cheng HL, Jedrychowski MP, Gygi SP, Sinclair DA, Alt FW, Greenberg ME. Stress-dependent regulation of FOXO transcription factors by the SIRT1 deacetylase. *Science*. 2004;303:2011–2015.
8. Daitoku H, Hatta M, Matsuzaki H, Aratani S, Ohshima T, Miyagishi M, Nakajima T, Fukamizu A. Silent information regulator 2 potentiates Foxo1-mediated transcription through its deacetylase activity. *Proc Natl Acad Sci U S A*. 2004;101:10042–10047.
9. Brooks CL, Gu W. Ubiquitination, phosphorylation and acetylation: the molecular basis for p53 regulation. *Curr Opin Cell Biol*. 2003;15:164–171.
10. Picard F, Kurtev M, Chung N, Topark-Ngarm A, Senawong T, Machado De Oliveira R, Leid M, McBurney MW, Guarente L. Sirt1 promotes fat mobilization in white adipocytes by repressing PPAR-gamma. *Nature*. 2004;429:771–776.
11. Rodgers JT, Lerin C, Haas W, Gygi SP, Spiegelman BM, Puigserver P. Nutrient control of glucose homeostasis through a complex of PGC-1alpha and SIRT1. *Nature*. 2005;434:113–118.
12. Nemoto S, Fergusson MM, Finkel T. SIRT1 functionally interacts with the metabolic regulator and transcriptional coactivator PGC-1{alpha}. *J Biol Chem*. 2005;280:16456–16460.
13. Bordone L, Motta MC, Picard F, Robinson A, Jhala US, Apfeld J, McDonagh T, Lemieux M, McBurney M, Szilvasi A, Easlon EJ, Lin SJ, Guarente L. Sirt1 regulates insulin secretion by repressing UCP2 in pancreatic beta cells. *PLoS Biol*. 2006;4:e31.
14. Moynihan KA, Grimm AA, Plueger MM, Bernal-Mizrachi E, Ford E, Cras-Meneur C, Permutt MA, Imai S. Increased dosage of mammalian Sir2 in pancreatic beta cells enhances glucose-stimulated insulin secretion in mice. *Cell Metab*. 2005;2:105–117.
15. Sun C, Zhang F, Ge X, Yan T, Chen X, Shi X, Zhai Q. SIRT1 improves insulin sensitivity under insulin-resistant conditions by repressing PTP1B. *Cell Metab*. 2007;6:307–319.
16. Baur JA, Pearson KJ, Price NL, Jamieson HA, Lerin C, Kalra A, Prabhu VV, Allard JS, Lopez-Lluch G, Lewis K, Pistell PJ, Poosala S, Becker KG, Boss O, Gwinn D, Wang M, Ramaswamy S, Fishbein KW, Spencer RG, Lakatta EG, Le Couteur D, Shaw RJ, Navas P, Puigserver P, Ingram DK, de Cabo R, Sinclair DA. Resveratrol improves health and survival of mice on a high-calorie diet. *Nature*. 2006;444:337–342.
17. Lagouge M, Argmann C, Gerhart-Hines Z, Meziane H, Lerin C, Daussin F, Messadeq N, Milne J, Lambert P, Elliott P, Geny B, Laakso M, Puigserver P, Auwerx J. Resveratrol improves mitochondrial function and protects against metabolic disease by activating SIRT1 and PGC-1alpha. *Cell*. 2006;127:1109–1122.
18. Pearson KJ, Baur JA, Lewis KN, Peshkin L, Price NL, Labinskyy N, Swindell WR, Kamara D, Minor RK, Perez E, Jamieson HA, Zhang Y, Dunn SR, Sharma K, Pleshko N, Woollett LA, Csiszar A, Ikeno Y, Le

Couteur D, Elliott PJ, Becker KG, Navas P, Ingram DK, Wolf NS, Ungvari Z, Sinclair DA, de Cabo R. Resveratrol delays age-related deterioration and mimics transcriptional aspects of dietary restriction without extending life span. *Cell Metab.* 2008;8:157–168.
19. Potente M, Ghaeni L, Baldessari D, Mostoslavsky R, Rossig L, Dequiedt F, Haendeler J, Mione M, Dejana E, Alt FW, Zeiher AM, Dimmeler S. SIRT1 controls endothelial angiogenic functions during vascular growth. *Genes Dev.* 2007;21:2644–2658.
20. Minamino T, Komuro I. Vascular cell senescence: contribution to atherosclerosis. *Circ Res.* 2007;100:15–26.
21. Chen J, Goligorsky MS. Premature senescence of endothelial cells: Methusaleh's dilemma. *Am J Physiol Heart Circ Physiol.* 2006;290: H1729–1739.
22. Minamino T, Miyauchi H, Yoshida T, Ishida Y, Yoshida H, Komuro I. Endothelial cell senescence in human atherosclerosis: role of telomere in endothelial dysfunction. *Circulation.* 2002;105:1541–1544.
23. Brodsky SV, Gealekman O, Chen J, Zhang F, Togashi N, Crabtree M, Gross SS, Nasjletti A, Goligorsky MS. Prevention and reversal of premature endothelial cell senescence and vasculopathy in obesity-induced diabetes by ebselen. *Circ Res.* 2004;94:377–384.
24. Ota H, Tokunaga E, Chang K, Hikasa M, Iijima K, Eto M, Kozaki K, Akishita M, Ouchi Y, Kaneki M. Sirt1 inhibitor, Sirtinol, induces senescence-like growth arrest with attenuated Ras-MAPK signaling in human cancer cells. *Oncogene.* 2006;25:176–185.
25. Howitz KT, Bitterman KJ, Cohen HY, Lamming DW, Lavu S, Wood JG, Zipkin RE, Chung P, Kisielewski A, Zhang LL, Scherer B, Sinclair DA. Small molecule activators of sirtuins extend Saccharomyces cerevisiae lifespan. *Nature.* 2003;425:191–196.
26. Baur JA, Sinclair DA. Therapeutic potential of resveratrol: the in vivo evidence. *Nat Rev Drug Discov.* 2006;5:493–506.
27. Nemoto S, Fergusson MM, Finkel T. Nutrient availability regulates SIRT1 through a forkhead-dependent pathway. *Science.* 2004;306: 2105–2108.
28. Sheu ML, Ho FM, Yang RS, Chao KF, Lin WW, Lin-Shiau SY, Liu SH. High glucose induces human endothelial cell apoptosis through a phosphoinositide 3-kinase-regulated cyclooxygenase-2 pathway. *Arterioscler Thromb Vasc Biol.* 2005;25:539–545.
29. Clodfelder-Miller B, De Sarno P, Zmijewska AA, Song L, Jope RS. Physiological and pathological changes in glucose regulate brain Akt and glycogen synthase kinase-3. *J Biol Chem.* 2005;280:39723–39731.
30. Greer EL, Oskoui PR, Banko MR, Maniar JM, Gygi MP, Gygi SP, Brunet A. The energy sensor AMP-activated protein kinase directly regulates the mammalian FOXO3 transcription factor. *J Biol Chem.* 2007;282: 30107–30119.
31. Tang Y, Zhao W, Chen Y, Zhao Y, Gu W. Acetylation is indispensable for p53 activation. *Cell.* 2008;133:612–626.
32. Ito A, Lai CH, Zhao X, Saito S, Hamilton MH, Appella E, Yao TP. p300/CBP-mediated p53 acetylation is commonly induced by p53-activating agents and inhibited by MDM2. *EMBO J.* 2001;20:1331–1340.
33. Miyauchi H, Minamino T, Tateno K, Kunieda T, Toko H, Komuro I. Akt negatively regulates the in vitro lifespan of human endothelial cells via a p53/p21-dependent pathway. *Embo J.* 2004;23:212–220.
34. Brownlee M. Biochemistry and molecular cell biology of diabetic complications. *Nature.* 2001;414:813–820.
35. Gorgoulis VG, Zacharatos P, Kotsinas A, Kletsas D, Mariatos G, Zoumpourlis V, Ryan KM, Kittas C, Papavassiliou AG. p53 activates ICAM-1 (CD54) expression in an NF-kappaB-independent manner. *Embo J.* 2003;22:1567–1578.

Cardiac 12/15 lipoxygenase–induced inflammation is involved in heart failure

Yosuke Kayama,[1,4] Tohru Minamino,[1,2] Haruhiro Toko,[1] Masaya Sakamoto,[3] Ippei Shimizu,[1] Hidehisa Takahashi,[1] Sho Okada,[1] Kaoru Tateno,[1] Junji Moriya,[1] Masataka Yokoyama,[1] Aika Nojima,[1] Michihiro Yoshimura,[4] Kensuke Egashira,[5] Hiroyuki Aburatani,[6] and Issei Komuro[1]

[1]Department of Cardiovascular Science and Medicine, Chiba University Graduate School of Medicine, Chuo-ku, Chiba 260-8670, Japan
[2]PRESTO, Japan Science and Technology Agency, Saitama 332-0012, Japan
[3]Department of Diabetes, Metabolism and Endocrinology and [4]Department of Cardiology, Jikei University School of Medicine, Minato-ku, Tokyo 105-8461, Japan
[5]Department of Cardiovascular Medicine, Graduate School of Medical Sciences, Kyushu University, Higashi-ku, Fukuoka 812-8582, Japan
[6]Genome Science Division, Research Center for Advanced Science and Technology, University of Tokyo, Meguro-ku, Tokyo 153-8904, Japan

To identify a novel target for the treatment of heart failure, we examined gene expression in the failing heart. Among the genes analyzed, *Alox15* encoding the protein 12/15 lipoxygenase (LOX) was markedly up-regulated in heart failure. To determine whether increased expression of 12/15-LOX causes heart failure, we established transgenic mice that overexpressed 12/15-LOX in cardiomyocytes. Echocardiography showed that *Alox15* transgenic mice developed systolic dysfunction. Cardiac fibrosis increased in *Alox15* transgenic mice with advancing age and was associated with the infiltration of macrophages. Consistent with these observations, cardiac expression of monocyte chemoattractant protein 1 (MCP-1) was up-regulated in *Alox15* transgenic mice compared with wild-type mice. Treatment with 12-hydroxy-eicosatetraenoic acid, a major metabolite of 12/15-LOX, increased MCP-1 expression in cardiac fibroblasts and endothelial cells but not in cardiomyocytes. Inhibition of MCP-1 reduced the infiltration of macrophages into the myocardium and prevented both systolic dysfunction and cardiac fibrosis in *Alox15* transgenic mice. Likewise, disruption of 12/15-LOX significantly reduced cardiac MCP-1 expression and macrophage infiltration, thereby improving systolic dysfunction induced by chronic pressure overload. Our results suggest that cardiac 12/15-LOX is involved in the development of heart failure and that inhibition of 12/15-LOX could be a novel treatment for this condition.

CORRESPONDENCE
Issei Komuro:
komuro-tky@umin.ac.jp

Abbreviations used: cDNA, complementary DNA; FS, fractional shortening; HETE, hydroxy-eicosatetraenoic acids; LOX, lipoxygenase; LVDd, left ventricular diastolic dimension; MCP-1, monocyte chemoattractant protein 1; mRNA, messenger RNA; TAC, transverse aortic constriction.

Heart failure is a clinical syndrome that is associated with various cardiovascular diseases such as hypertension and myocardial infarction (Libby and Braunwald, 2008). Comprehensive management using current therapeutic options can markedly reduce the morbidity and mortality of heart failure. Large-scale clinical trials of drugs targeting neurohormonal mechanisms, such as angiotensin-converting enzyme inhibitors and β blockers, have shown that such treatment is effective for reducing mortality in patients with heart failure (Garg and Yusuf, 1995; McMurray, 1999; Goldstein, 2002). However, heart failure is still one of the leading causes of death worldwide (Libby and Braunwald, 2008), so it is important to investigate the underlying mechanisms of this condition and develop more effective treatments.

Arachidonic acid is a free fatty acid that, when liberated from cell membranes, can be metabolized by cyclooxygenase, cytochrome p450, and lipoxygenase (LOX) to form biologically active products such as prostaglandins, leukotrienes, and hydroxy-eicosatetraenoic acids (HETEs;

Y. Kayama, T. Minamino, and H. Toko contributed equally to this paper.

The Rockefeller University Press $30.00
J. Exp. Med. Vol. 206 No. 7 1565-1574
www.jem.org/cgi/doi/10.1084/jem.20082596

Kudo and Murakami, 2002). LOXs are a family of lipid-peroxidizing enzymes that oxidize free and esterified polyenolic fatty acids to form the corresponding hydroperoxy derivates (Kuhn and O'Donnell, 2006). The LOX enzymes are named according to the specific carbon atoms of arachidonic acid that are oxidized. Thus, 12/15-LOX is a member of the LOX family that catalyzes the step from arachidonic acid to 12(S)-HETE and 15(S)-HETE (Chen et al., 1994). 12/15-LOX was originally isolated from porcine leukocytes (Yokoyama et al., 1986), but its tissue distribution is now known to be relatively wide, including blood vessels, the brain, and the kidneys (Kuhn and O'Donnell, 2006). Several lines of evidence have suggested that 12/15-LOX may play an important role in the development of atherosclerosis, diabetes, and neurodegenerative disease (Natarajan and Nadler, 2004; Kuhn and O'Donnell, 2006). For example, disruption of the gene for 12/15-LOX in mice significantly reduces the onset of atherosclerosis (Cyrus et al., 1999, 2001; George et al., 2001), whereas an increase of 12/15-LOX expression in mice promotes monocyte–endothelial cell interactions that lead to atherogenesis (Hatley et al., 2003; Reilly et al., 2004; Bolick et al., 2005). Several studies have shown that monocyte 12/15-LOX mediates the oxidative modification of low-density lipoprotein (McNally et al., 1990; Sakashita et al., 1999; Zhu et al., 2003b). An increase of 12/15-LOX activity in vessel walls also contributes to atherogenesis by impairing the macrophage cholesterol efflux pathway (Nagelin et al., 2008). Interestingly, mice with deficiency of 12/15-LOX are resistant to the development of streptozotocin-induced diabetes (Bleich et al., 1999) and autoimmune diabetes (McDuffie et al., 2008). However, there is currently little evidence that 12/15-LOX has a role in heart failure.

In the present study, we showed that cardiac 12/15-LOX induces inflammation that is involved in heart failure. We found that 12/15-LOX expression was markedly increased in the failing heart. Increased expression of this enzyme up-regulates monocyte chemoattractant protein 1 (MCP-1) and promotes the infiltration of macrophages into the heart, thereby causing cardiac fibrosis and systolic dysfunction. Conversely, disruption of *Alox15* reduces cardiac MCP-1 expression and macrophage infiltration, thereby improving systolic dysfunction induced by chronic pressure overload. These findings suggest that inhibition of 12/15-LOX could be a novel treatment for heart failure.

RESULTS

Increased expression of 12/15-LOX causes heart failure

To clarify the molecular mechanisms of heart failure, we performed microarray analysis using cardiac tissue samples obtained from a hypertensive heart failure model (Dahl salt-sensitive rats). Approximately 300 genes showed significant changes of expression in failing hearts compared with control hearts. For example, fetal genes, such as the natriuretic peptide genes and the β-type myosin heavy chain gene, were up-regulated, whereas cardioprotective genes, such as heat shock proteins, were down-regulated (Table S1). Among the genes analyzed, *Alox15* encoding the protein 12/15-LOX was most markedly up-regulated in failing hearts compared with control hearts (Fig. 1 A). Northern blot analysis confirmed that the messenger RNA (mRNA) for this gene was strikingly elevated in heart failure (Fig. 1 B). Immunohistochemistry showed that expression of 12/15-LOX was specifically up-regulated in cardiomyocytes of failing hearts (Fig. 1 C).

To determine whether increased expression of 12/15-LOX could cause heart failure, we established *Alox15* transgenic mice in which expression of the murine *Alox15* gene was under the control of the α-cardiac myosin heavy chain promoter. We obtained two lines of transgenic mice, both of which showed an ~10-fold increase in the myocardial expression of 12/15-LOX compared with their WT littermates (Fig. 2 A; and Fig. S1, A and B). Histological examination also indicated that the transgenic mice showed increased myocardial expression of 12/15-LOX (Fig. 2 B and Fig. S1 C). Consequently, production of 12(S)-HETE and 15(S)-HETE was significantly increased in the hearts of *Alox15* transgenic mice (Fig. 2 C). The left ventricular diastolic dimension (LVDd) was increased and left ventricular fractional shortening (FS) was decreased in *Alox15* transgenic mice from 26 wk of age compared with their WT littermates (Fig. 2 D). These changes observed in the transgenic animals showed further progression with aging (Fig. 2 D). Histological examination revealed that cardiac fibrosis was increased in *Alox15* transgenic mice and that this fibrosis also progressed with advancing age and was associated with infiltration of macrophages (Fig. 2, E and F). There was no difference in blood pressure between *Alox15* transgenic mice and their WT littermates at 16 or 48 wk of age (Fig. S1 D). The cardiac changes were similar in two independent lines of *Alox15* transgenic mice, suggesting that increased expression of 12/15-LOX might cause heart failure by inducing myocardial inflammation.

12/15-LOX induces cardiac inflammation

To investigate the mechanism by which cardiac infiltration of macrophages was increased in *Alox15* transgenic mice, we examined the expression of various proinflammatory cytokines that are thought to be macrophage chemoattractants by the ribonuclease protection assay. We found that cardiac expression of *Ccl2* (MCP-1) was significantly increased in *Alox15* transgenic mice compared with WT mice (Fig. 3 A). In vitro experiments demonstrated that treatment with 12(S)-HETE increased *Ccl2* expression by cardiac fibroblasts and endothelial cells (Fig. 3, B and C), whereas there was no effect when cardiomyocytes were treated with 12(S)-HETE (Fig. 3 D). Moreover, incubation of COS7 cells with 12(S)-HETE significantly increased the activity of nuclear factor κB, a transcription factor that regulates the induction of proinflammatory cytokines including MCP-1 (Fig. 3 E). In contrast, 12(S)-HETE did not affect the activity of this factor when cells were transfected with a reporter plasmid containing mutant κB binding sites (Fig. 3 E). These results suggest that increased production of 12(S)-HETE by cardiomyocytes

Published July 6, 2009

causes up-regulation of MCP-1 in other cells of the heart, thereby leading to accumulation of macrophages.

To investigate the relationship between up-regulation of MCP-1 and heart failure, we examined the effect of MCP-1 inhibition on cardiac dysfunction in *Alox15* transgenic mice. We injected an expression vector encoding mutant human MCP-1 with deletion of N-terminal amino acids (7ND plasmid; Egashira, 2003) or the empty vector (mock) into the thigh muscles of mice every 2 wk until 48 wk of age. The result was a significant increase in the blood level of 7ND and elevation of plasma human MCP-1 (Fig. 4 A and Fig. S2). This mutant MCP-1 binds to the MCP-1 receptor (chemokine receptor 2) and inhibits downstream signaling (Egashira, 2003). Consequently, injection of the 7ND plasmid has been reported to suppress MCP-1 activity in vivo and inhibit the development of atherosclerosis (Ni et al., 2001), as well as inhibiting cardiac remodelling after myocardial infarction (Hayashidani et al., 2003). In agreement with these results,

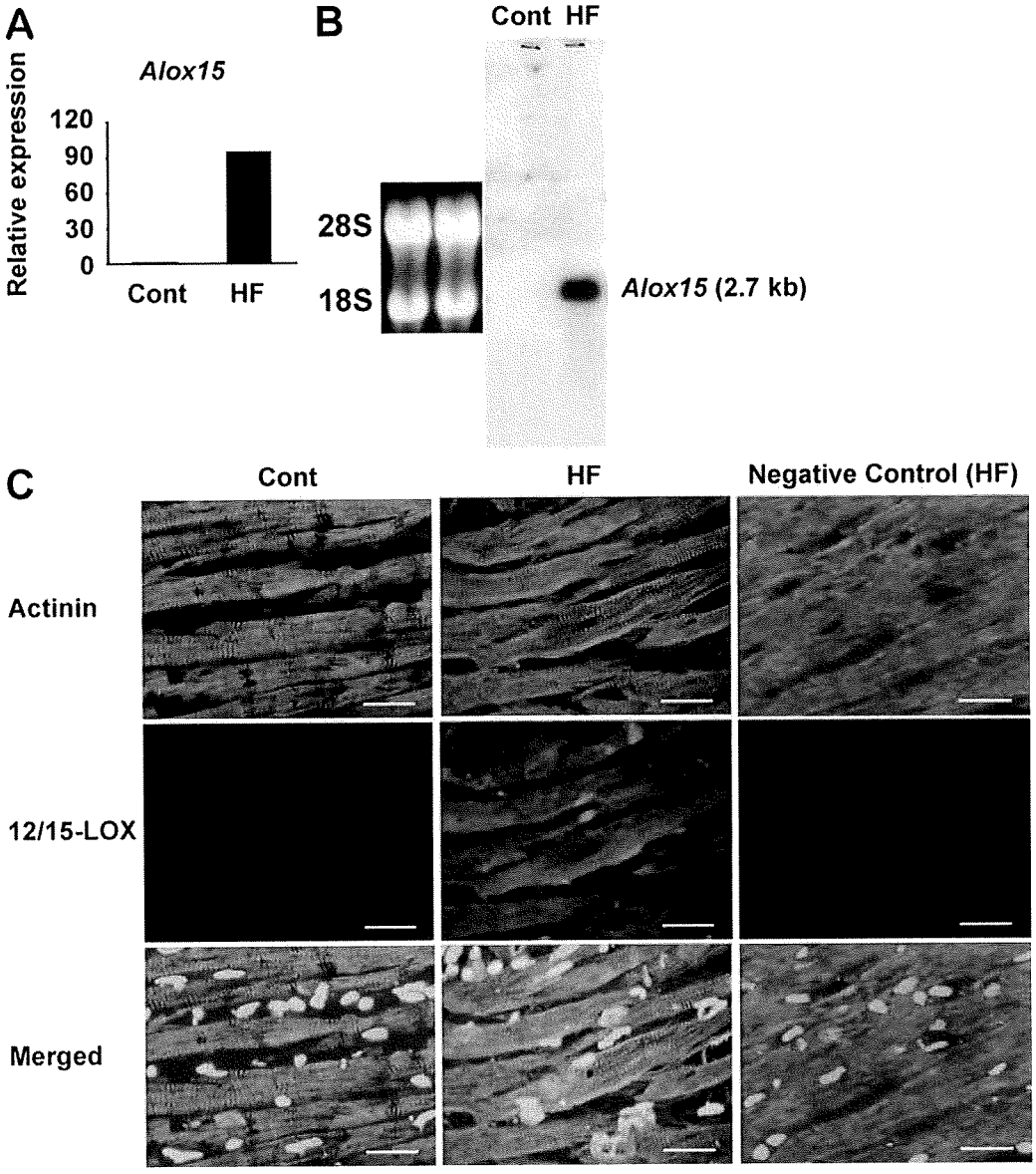

Figure 1. Expression of 12/15-LOX is up-regulated in the failing heart. (A) Dahl salt-sensitive rats were fed a low-sodium diet until the age of 6 wk and then a high-sodium diet (8% NaCl) throughout the experimental period. In this model, prominent cardiac hypertrophy developed and left ventricular systolic function was impaired by 17 wk of age. Rats fed a low-salt diet (0.3% NaCl) served as the control. The animals were sacrificed for gene chip analysis at 17 wk of age. Expression of *Alox15* was markedly up-regulated in failing hearts (HF) compared with control hearts (Cont). (B) Northern blot analysis confirmed that the expression of mRNA for *Alox15* was strikingly elevated in failing hearts. (C) Immunohistochemistry for 12/15-LOX in the heart at 17 wk of age. Expression of 12/15-LOX (red) was specifically up-regulated in cardiomyocytes (green) of failing hearts. Nuclei were stained with DAPI (blue). Bars, 20 µm. Normal rabbit serum was used as a negative control of polyclonal antibody against 12/15-LOX. Results in A are obtained from one experiment. Results in B and C are representative of three independent experiments.

Supplemental Material can be found at:
http://jem.rupress.org/content/suppl/2009/06/22/jem.20082596.DC1.html

Published July 6, 2009

JEM

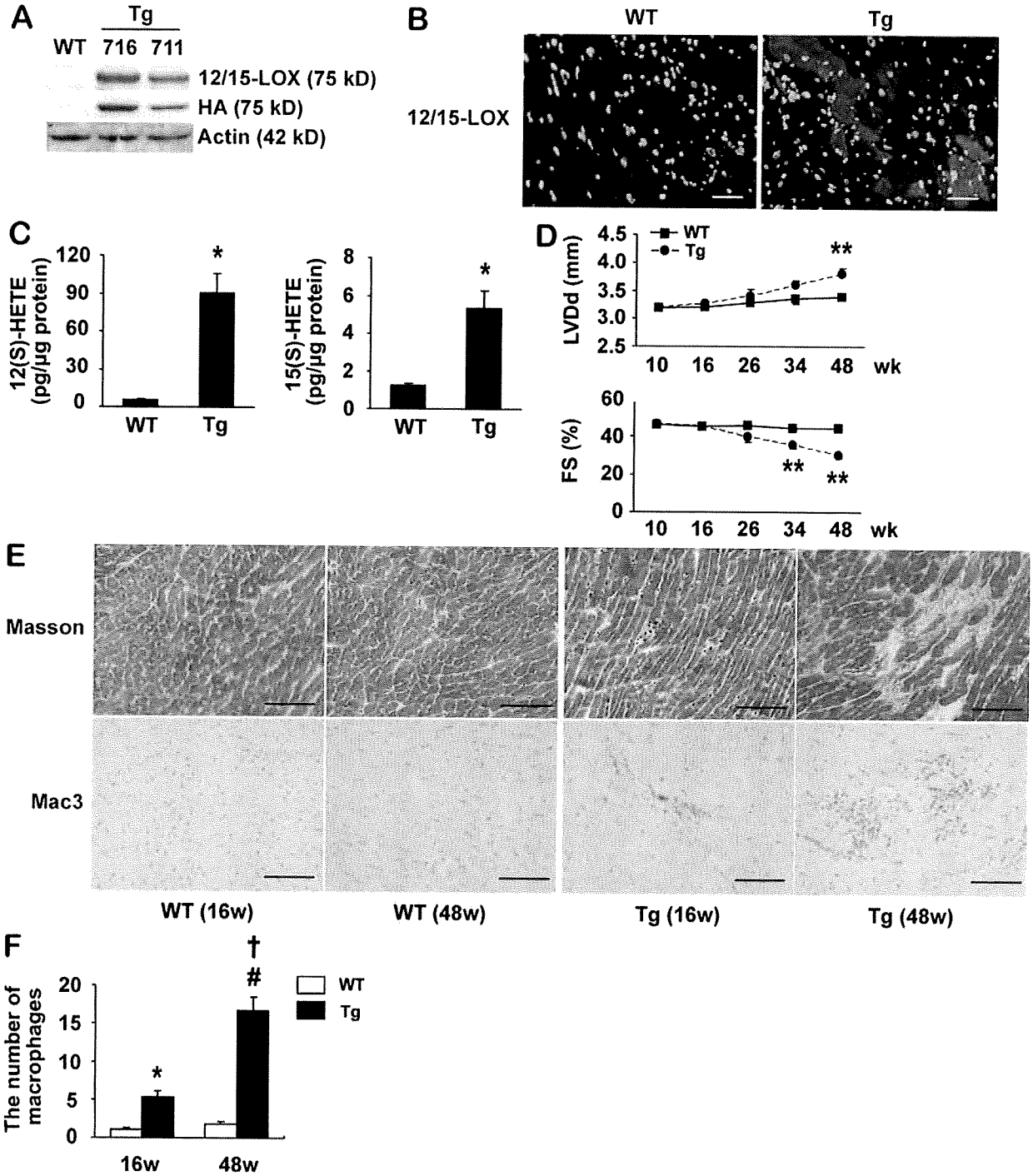

Figure 2. Increased expression of 12/15-LOX causes heart failure. (A) Western blot analysis of 12/15-LOX expression in the hearts of WT and *Alox15* transgenic (Tg) mice using anti-12/15-LOX antibody (12/15-LOX) or anti-HA antibody (HA). (B) Immunohistochemistry for 12/15-LOX (red) in the hearts of WT and *Alox15* transgenic mice. Nuclei were stained with DAPI (blue). Bars, 40 μm. Results in A and B are representative of three independent experiments. (C) 12/15(S)-HETE levels in the hearts of WT and *Alox15* transgenic mice. (D) Echocardiographic findings in WT and transgenic mice. The LVDd was increased and left ventricular FS was decreased in *Alox15* transgenic mice compared with their WT littermates. These changes observed in the transgenic animals showed progression with aging. *, $P < 0.05$; **, $P < 0.01$ versus WT. Results in C and D represent the mean ± SEM of three independent experiments. C, $n = 6$; D, $n = 14$. (E) Masson trichrome staining (top) and immunohistochemistry for Mac3 (bottom) in the hearts of WT and transgenic mice at the ages of 16 wk (16w) and 48 wk (48w). Cardiac fibrosis was increased in *Alox15* transgenic mice, and this fibrosis progressed with advancing age and was associated with infiltration of macrophages. Bars, 100 μm. Results are representative of three independent experiments. (F) The number of Mac3-positive cells in the hearts of WT and transgenic mice at the ages of 16 wk (16w) and 48 wk (48w). *, $P < 0.01$ versus WT (16w); #, $P < 0.01$ versus WT (48w); †, $P < 0.01$ versus transgenic (16w). Results represent the mean ± SEM of three independent experiments; $n = 7$.

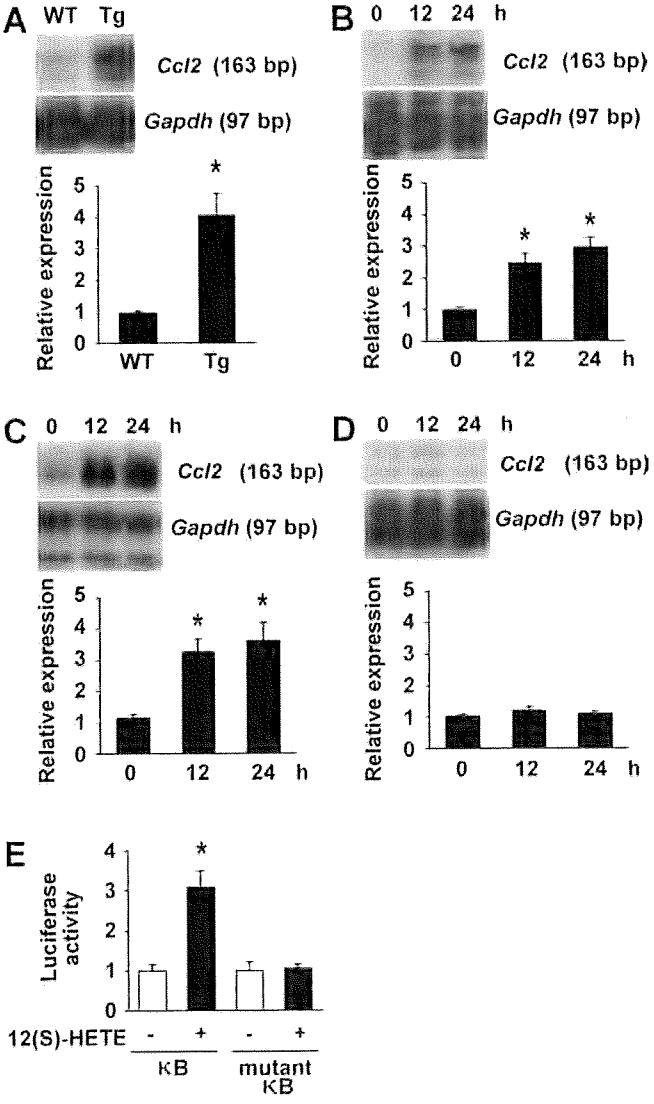

Figure 3. 12/15-LOX up-regulates MCP-1 expression. (A) Expression of *Ccl2* (MCP-1) was examined in the hearts of WT and *12/15-LOX* transgenic (Tg) mice by the ribonuclease protection assay. The graph indicates relative expression of *Ccl2*. Cardiac expression of *Ccl2* was significantly greater in *Alox15* transgenic mice than in WT mice. *, $P < 0.05$ versus WT. Results represent the mean ± SEM of three independent experiments; $n = 6$. (B–D) Cardiac fibroblasts (B), endothelial cells (C), and cardiomyocytes (D) were treated with 5×10^{-7} M 12(S)-HETE for the indicated times (0–24 h), and expression of *Ccl2* was examined by the ribonuclease protection assay. Graphs display relative expression of *Ccl2*. Incubation with 12(S)-HETE increased *Ccl2* expression by cardiac fibroblasts and endothelial cells. *, $P < 0.01$ versus time 0. Results represent mean ± SEM of four independent experiments; $n = 4$ for B and C; $n = 7$ for D. (E) The luciferase reporter gene plasmid containing the κB binding site was transfected into COS7 cells, which were cultured in the absence or presence of 5×10^{-7} M 12(S)-HETE. The luciferase assay was performed 12 h later. A reporter plasmid containing the mutant κB binding site was used as the negative control. Incubation of cells with 12(S)-HETE significantly increased the activity of nuclear factor κB. *, $P < 0.01$ versus 12(S)-HETE (−)/κB. Results represent the mean ± SEM of five independent experiments; $n = 6$.

histological examination and echocardiography demonstrated that injection of this plasmid reduced the myocardial infiltration of macrophages in *Alox15* transgenic mice, as well as preventing systolic dysfunction and left ventricular dilatation (Fig. 4, B and C). These results suggested that 12/15-LOX induces cardiac dysfunction by up-regulation of MCP-1 expression in the heart.

Cardiac expression of 12/15-LOX is up-regulated during pressure overload

To further investigate the role of 12/15-LOX in heart failure, we examined its cardiac expression in WT mice with severe transverse aortic constriction (TAC). In this model, cardiac hypertrophy gradually progresses to reach a peak on day 7 after TAC and then decreases afterward (not depicted). FS was preserved until day 7 but was significantly decreased on day 14 along with left ventricular dilatation (Fig. 5 A). Cardiac expression of *Alox15* was significantly up-regulated after TAC (Fig. 5 B), and the production of both 12(S)-HETE and 15(S)-HETE was increased in the heart (Fig. 5 C). Histological examination demonstrated an increase in the expression of 12/15-LOX by cardiomyocytes after TAC (Fig. 6 A and Fig. S3).

We next created *Alox15*-deficient mice with TAC and compared them to WT TAC mice. The increase of 12(S)-HETE and 15(S)-HETE production after TAC was markedly attenuated by disruption of *Alox15* (Fig. 6). Disruption of *Alox15* also significantly improved systolic dysfunction and prevented left ventricular dilatation in the presence of chronic pressure overload without any change of blood pressure (Fig. 5 A and Fig. S4), indicating that 12/15-LOX has an important role in the induction of cardiac dysfunction by pressure overload. To examine whether *Alox15* deficiency could inhibit cardiac inflammation, we assessed the expression of *Ccl2* and a macrophage marker (Cd68) in the heart after TAC. Expression of both genes was increased by about threefold at 14 d after TAC. The increase of *Ccl2* and *Cd68* expression was significantly inhibited by disruption of *Alox15* (Fig. 6 C), suggesting that this gene has a crucial role in the development of heart failure by promoting cardiac inflammation.

DISCUSSION

We demonstrated a crucial role of 12/15-LOX–induced inflammation in the development of heart failure. Activation of this enzyme has been shown to promote neuronal death, whereas inhibition of 12/15-LOX protects against brain damage caused by oxidative stress or ischemia by inhibiting neuronal death (Lebeau et al., 2004; Jin et al., 2008; Seiler et al., 2008). In contrast, treatment with 12(S)-HETE does not induce the apoptosis of cultured cardiomyocytes (unpublished data). Indeed, few apoptotic cardiomyocytes were detected in the hearts of *Alox15* transgenic mice even after the onset of systolic dysfunction (unpublished data). Instead, these mice showed an increase of macrophages infiltrating into the myocardium, which was associated with cardiac fibrosis and systolic dysfunction. Our findings suggested that MCP-1 may

Published July 6, 2009

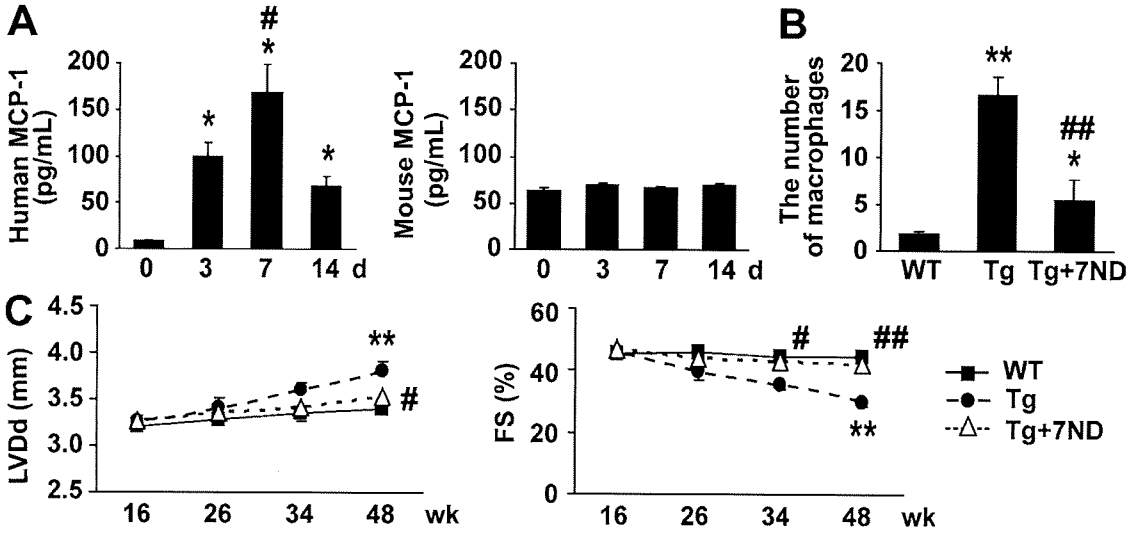

Figure 4. Inhibition of MCP-1 prevents cardiac dysfunction in *Alox15* transgenic animals. (A) The plasma levels of 7ND (human MCP-1) and murine MCP-1 were determined by ELISA at the indicated times after introduction of the 7ND expression vector. The plasma level of human MCP-1 was significantly increased after injection of the 7ND plasmid. *, $P < 0.01$ versus day 0; #, $P < 0.01$ versus day 3. Results represent the mean ± SEM of three independent experiments; $n = 5$. (B) Number of Mac3-positive cells in the hearts of WT mice, transgenic (Tg) mice, and transgenic mice treated with 7ND (Tg + 7ND). Injection of the 7ND plasmid reduced the myocardial infiltration of macrophages in *Alox15* transgenic mice. (C) Echocardiographic findings in WT mice, transgenic mice, and transgenic mice treated with 7ND (Tg + 7ND). Injection of the 7ND plasmid prevented systolic dysfunction and left ventricular dilatation in *Alox15* transgenic mice. *, $P < 0.05$; **, $P < 0.01$ versus WT; #, $P < 0.05$; ##, $P < 0.01$ versus transgenic. Results represent mean ± SEM of three independent experiments. B, $n = 7$; C, $n = 10$–14.

have a major role in promoting cardiac inflammation in *Alox15* transgenic mice because its inhibition almost completely abolished the accumulation of macrophages and prevented systolic dysfunction. We also showed that 12/15-LOX induces up-regulation of MCP-1 expression in the setting of pressure overload, thereby increasing cardiac inflammation and leading to systolic dysfunction. Consistent with our findings, inhibition of MCP-1 has been reported to attenuate

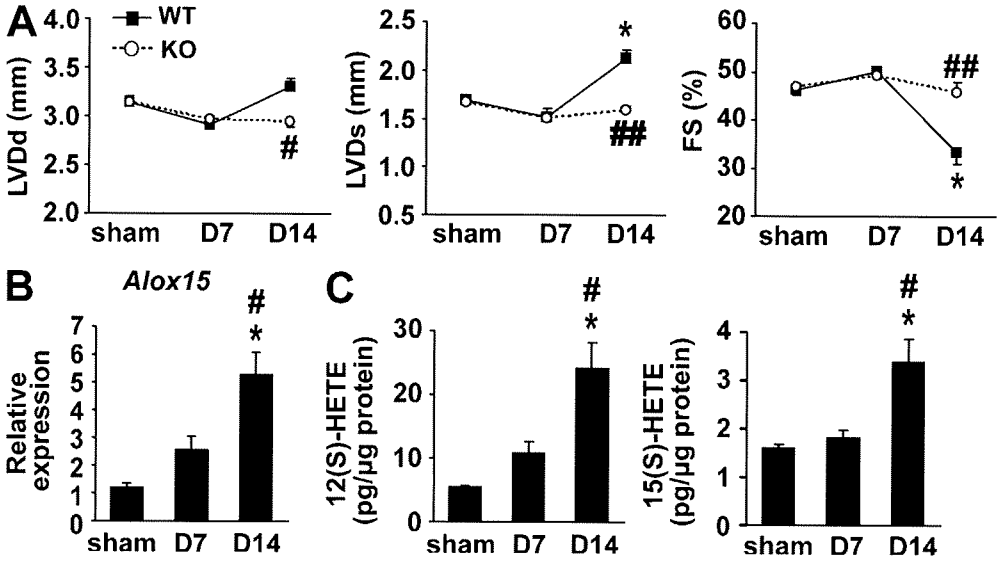

Figure 5. Cardiac expression of 12/15-LOX is up-regulated during pressure overload. (A) Echocardiographic findings in WT and *Alox15*-deficient (KO) mice on day 7 (D7) and day 14 (D14) after TAC surgery. FS was preserved until day 7 but was significantly decreased on day 14 along with left ventricular dilatation in WT mice. Disruption of *Alox15* (KO) significantly improved systolic dysfunction and prevented left ventricular dilatation caused by chronic pressure overload. LVDs, left ventricular systolic dimension; sham, sham operation. *, $P < 0.01$ versus sham; #, $P < 0.05$; ##, $P < 0.01$ versus WT. Results represent the mean ± SEM of three independent experiments; $n = 10$. (B and C) *Alox15* expression (B) and the 12/15(S)-HETE level (C) were examined in the hearts of WT mice on day 7 (D7) and day 14 (D14) after TAC surgery by real-time PCR and ELISA, respectively. Cardiac expression of 12/15-LOX was significantly up-regulated after TAC, and production of both 12(S)-HETE and 15(S)-HETE was increased in the heart. *, $P < 0.01$ versus sham; #, $P < 0.01$ versus D7. Results represent the mean ± SEM of three independent experiments; $n = 6$.

Published July 6, 2009

myocardial inflammation, fibrosis, and cardiac dysfunction induced by chronic pressure overload (Kuwahara et al., 2004). It has also been reported that transgenic animals with cardiac expression of MCP-1 develop myocardial fibrosis and systolic dysfunction (Kolattukudy et al., 1998). In agreement with our in vitro data, it has been reported that MCP-1 expression is up-regulated in vascular endothelial cells and fibroblasts by pressure overload (Kuwahara et al., 2004). Collectively, these

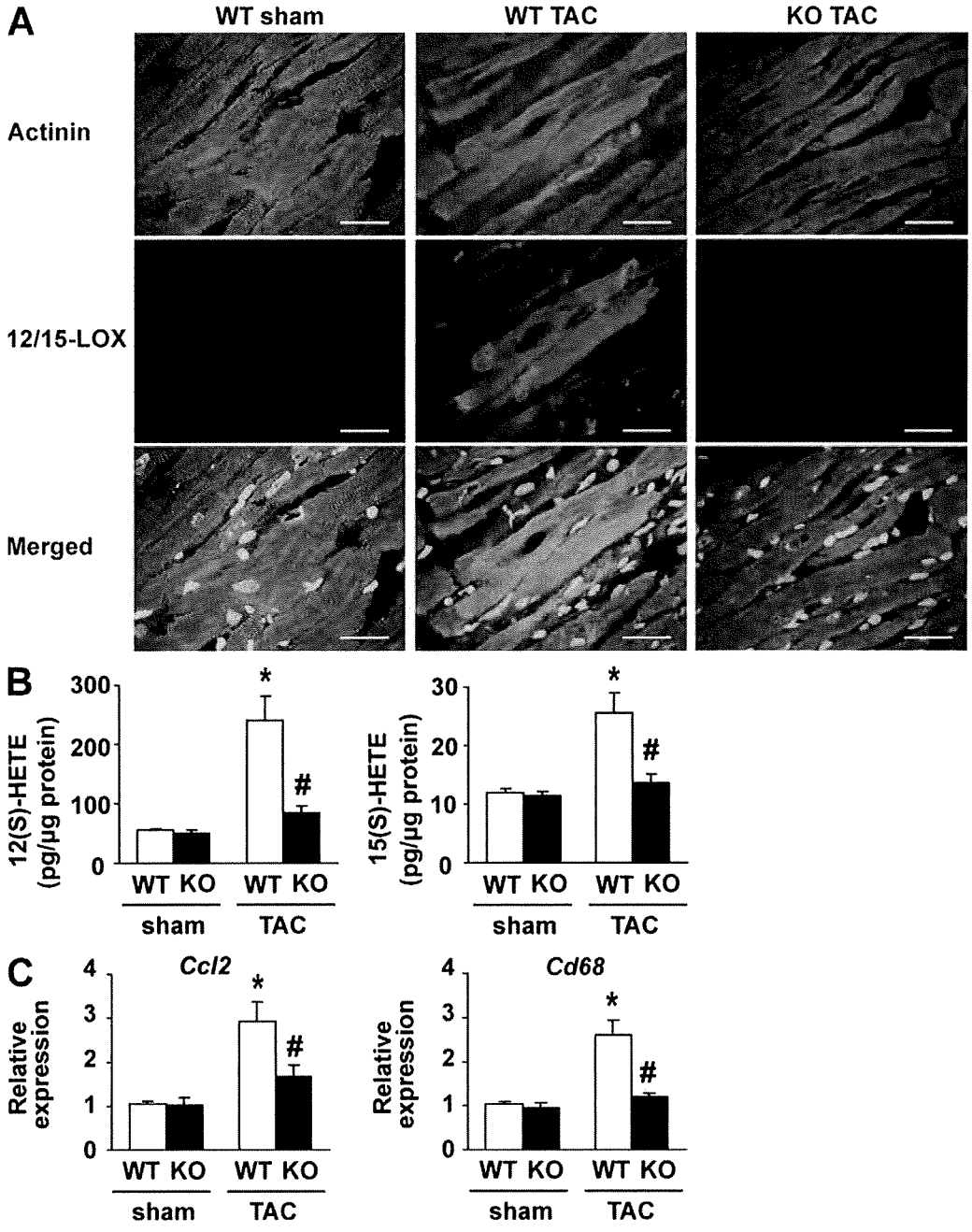

Figure 6. Disruption of *Alox15* attenuates cardiac inflammation during pressure overload. (A) Double immunostaining for 12/15-LOX (red) and actinin (green) in the hearts of sham-operated WT mice (WT sham), WT mice with TAC (WT TAC), and *Alox15*-deficient mice with TAC (KO TAC). Increased expression of 12/15-LOX was observed in cardiomyocytes after TAC in WT mice but not KO mice. Nuclei were stained with DAPI (blue). Bars, 20 μm. Results are representative of four independent experiments. (B) 12/15(S)-HETE levels were examined in the hearts of WT and *Alox15*-deficient (KO) mice after sham surgery or TAC. The increase of 12(S)-HETE and 15(S)-HETE production after TAC was markedly attenuated in *Alox15*-deficient mice (KO). *, $P < 0.01$ versus WT sham; #, $P < 0.01$ versus WT TAC. Results represent the mean ± SEM of three independent experiments; $n = 6–8$. (C) Expression of *Ccl2* (MCP-1) and *Cd68* was examined in the hearts of WT and *Alox15*-deficient (KO) mice after sham surgery or TAC. Expression of both genes was increased by about threefold at 14 d after TAC. This increase of expression was significantly inhibited by disruption of *Alox15*. *, $P < 0.01$ versus WT sham; #, $P < 0.01$ versus WT TAC. Results represent the mean ± SEM of three independent experiments; $n = 6–8$.

results indicate that chronic pressure overload increases the expression of 12/15-LOX, which then causes heart failure by promoting cardiac inflammation and fibrosis.

Target gene disruption or overexpression of 12/15-LOX in mice with a genetic background of apolipoprotein E or low-density lipoprotein receptor deficiency has shown that this enzyme may have a role in atherogenesis. The data indirectly support a role for 12/15-LOX in the oxidative modification of low-density lipoprotein. Consistent with our results, recent evidence suggests that 12/15-LOX plays a crucial role in the regulation of proinflammatory molecules and that this regulatory activity of 12/15-LOX may be important for linking 12/15-LOX activation to atherogenesis. For example, 12(S)-HETE increases the expression of MCP-1, interleukin 6, tumor necrosis factor α, and adhesion molecules by macrophages and vascular cells (Bolick et al., 2005, 2006; Wen et al., 2007, 2008; Dwarakanath et al., 2008), and these changes are partly mediated by activation of nuclear factor κB (Bolick et al., 2005, 2006; Dwarakanath et al., 2008). Disruption of 12/15-LOX has also been shown to attenuate airway allergic inflammation by modulating the expression of proinflammatory cytokines (Andersson et al., 2008).

The mechanism of 12/15-LOX activation in the failing heart is unclear. We previously demonstrated that mismatch between the number of capillaries and the size of cardiomyocytes occurs during the development of cardiac hypertrophy, leading to myocardial hypoxia and systolic dysfunction (Sano et al., 2007). Because exposure of cultured cardiomyocytes to hypoxia up-regulates 12/15-LOX expression (unpublished data), a hypoxic state might be one reason for the induction of 12/15-LOX in the failing heart. This concept is supported by previous results that hypoxia up-regulates 12/15-LOX expression in the lungs and the brain (Bernaudin et al., 2002; Zhu et al., 2003a). Moreover, we have found that 12/15-LOX expression is significantly up-regulated in the heart after myocardial infarction (unpublished data). There are putative binding elements for CCAAT/enhancer binding proteins and nuclear factor κB within the promoter region of the *Alox15* gene (unpublished data), and both of these molecules are known to be activated by hypoxia (Cummins and Taylor, 2005).

Inflammation has an important role in the pathogenesis and progression of many forms of heart failure, and biomarkers of inflammation have become the subject of intense investigation. In the Framingham Heart Study, an increase of C-reactive protein (as well as inflammatory cytokines such as interleukin 6 and tumor necrosis factor α) was found to identify asymptomatic older persons in the community with a high risk of developing heart failure in the future (Braunwald, 2008). Multivariate analysis has shown that an increase of C-reactive protein is an independent predictor of adverse outcomes in patients with acute or chronic heart failure (Anand et al., 2005), suggesting that heart failure is closely associated with systemic inflammation. Because metabolites of 12/15-LOX may have a role in vascular inflammation, insulin resistance, and renal dysfunction (Natarajan and Nadler, 2004; Kuhn and O'Donnell, 2006), activation of 12/15-LOX in the failing heart could induce systemic inflammation and have a detrimental effect on other inflammatory diseases such as atherosclerosis, metabolic syndrome, and nephropathy. Conversely, inhibition of 12/15-LOX could be an attractive new strategy for the treatment of heart failure, as well as various other inflammatory conditions.

MATERIALS AND METHODS

Animal models. All of the experimental protocols were approved by Chiba University review board. Male Dahl salt-sensitive (DS) rats were purchased from SLC. The rats were fed a low-sodium diet until the age of 6 wk and then a high-sodium diet (8% NaCl) throughout the experimental period. In this model, marked cardiac hypertrophy developed and left ventricular systolic function was impaired at 17 wk of age. Accordingly, DS rats were sacrificed for gene chip analysis at 17 wk. All of the DS rats given a high-sodium diet showed signs of heart failure such as rapid and labored respiration and diffuse left ventricular hypokinesis on echocardiography at the time of sacrifice. Other DS rats were fed a low-salt diet (0.3% NaCl) as a control group.

We generated transgenic mice on a C57BL/6 background that expressed 12/15-LOX in cardiomyocytes under the control of the α–cardiac myosin heavy chain (α-MHC) promoter. A mouse *Alox15* complementary DNA (cDNA) fragment (gift from C.D. Funk, University of Pennsylvania, Philadelphia, PA) fused with the HA tag was subcloned into the α-MHC promoter vector. The transgene was identified by genomic PCR with transgene-specific oligonucleotide primers (5′-CCACACCAGAAATGACAGAC-3′ and 5′-GCGGGCAGGGAGACAAGTAG-3′) and by Southern blot analysis. Two independent lines of *Alox15* transgenic mice (lines 711 and 716) were obtained. The cardiac phenotype was similar in both lines of transgenic animals. WT littermates were used as the control for all experiments.

Alox15-deficient mice on a C57BL/6 background were purchased from The Jackson Laboratory. WT littermates served as a control for all experiments. TAC was performed as described previously (Sano et al., 2007) on 10–11-wk-old male mice. Sham-operated mice underwent the same procedure without aorta constriction.

An expression vector encoding mutant human MCP-1 with deletion of N-terminal amino acids (7ND plasmid) was prepared as described elsewhere (Hayashidani et al., 2003). Under anesthesia, mice received an injection of 100 μg of either the empty vector or the 7ND plasmid in PBS into the bilateral tibial muscles using a 27-gauge needle fitted with a plastic collar that limited muscle penetration to ~5 mm. Injection was performed every 2 wk from 10 wk until 48 wk of age. To increase the efficiency of gene transfection, 100 μl of the myotoxic agent bupivacaine (0.25% wt/vol) was injected into the muscles 3 d before transfection. Transfection of 7ND leads to an increase of mutant MCP-1 in the blood, as indicated by elevation of its plasma concentration after 14 d. The circulating mutant MCP-1 binds to the receptor for MCP-1 (chemokine receptor 2) on target cells and effectively blocks MCP-1 signaling (Ni et al., 2001; Hayashidani et al., 2003).

Physiological and histological analysis. Echocardiography was performed with a Vevo 770 High Resolution Imaging System (Visual Sonics Inc.). To minimize variation of the data, the heart rate was ~500–600 beats per minute when cardiac function was assessed. The peak systolic blood pressure was recorded by a photoelectric pulse devise (Blood Pressure Meter BP-98A; Softron Co. Ltd.) placed on the tails of unanesthetized mice. Under anesthesia, a micropressure transducer with an outer diameter of 0.42 mm (Samba 201 control unit and Samba Preclin 420 transducer; Samba Sensors AB) was introduced into the right carotid artery. Pressure signals were recorded with a MacLab 3.6/s data acquisition system (AD Instruments) at a sampling rate of 2,000 Hz. 4-μm frozen cross sections of the heart were fixed in 4% paraformaldehyde and subjected to Masson trichrome staining or immunohistochemistry for Mac3 (BD). Digital photographs were taken at 400× magnification of 25 random fields from each heart, and the number of Mac3-positive cells was counted in each field. The frozen cardiac cross sections

were also stained with antibodies for 12/15-LOX (Cayman Chemical) and actinin (Sigma-Aldrich).

DNA chip analysis. 10 μg of total RNA was extracted from the left ventricles of rats by the Li-Urea method and was used to synthesize biotin-labeled cRNA, which was then hybridized to a high-density oligonucleotide array (Gene Chip U34A array; Affymetrix) according to the previously published protocol (Ishii et al., 2000). The array contains probe sets for ~8,800 genes and ESTs, which were selected from Build 34 of the UniGene Database (created from GenBank 107/dbEST 11/18/98). GeneChip 3.3 software (Affymetrix) was used to calculate the mean difference for each probe on the array, which showed the intensity of gene expression defined by Affymetrix using their algorithm. The mean difference has been shown to quantitatively reflect the abundance of a particular mRNA in a population. The data were deposited in GEO (GSM406556, GSM406557, and GSE16199).

RNA analysis. Total RNA was isolated from the hearts of mice with RNAZol-B (Molecular Research Center, Cincinnati, OH) and the ribonuclease protection assay (RiboQuant; BD) was performed according to the manufacturer's instructions. For Northern blot analysis, 30 μg of total RNA was separated on formaldehyde denaturing gel and transferred to a nylon membrane (GE Healthcare). Then the blot was hybridized with radiolabeled *Alox15* cDNA probe using Quickhyb hybridization solution (Agilent Technologies) according to the manufacturer's instructions. Rat *Alox15* cDNA fragment was a gift from T. Yoshimoto (Kanazawa University Graduate School of Medical Science, Kanazawa, Japan). Mouse *Alox12* cDNA fragment was a gift from C.D. Funk. Real-time PCR was performed using a LightCycler (Roche) with the Taqman Universal Probe Library and the Light Cycler Master (Roche) according to the manufacturer's instructions.

Western blot analysis. Whole cell lysates were prepared in lysis buffer (10 mM Tris-HCl, pH 8, 140 mM NaCl, 5 mM EDTA, 0.025% NaN_3, 1% Triton X-100, 1% deoxycholate, 0.1% SDS, 1 mM PMSF, 5 μg/ml leupeptin, 2 μg/ml aprotinin, 50 mM NaF, and 1 mM $Na2VO_3$). 40–50 μg of the lysates were resolved by SDS-PAGE (PAGE). Then proteins were transferred to a nitrocellulose membrane (GE Healthcare), which was incubated with the primary antibody, followed by anti–rabbit or anti–mouse immunoglobulin G conjugated with horseradish peroxidase (Jackson ImmunoResearch Laboratories). Specific proteins were detected by using enhanced chemiluminescence (GE Healthcare). The primary antibodies used for Western blotting were as follows: anti-HA antibody (Santa Cruz Biotechnology, Inc.), anti–12/15-LOX antibody (Cayman Chemical), and anti-actin antibody (Sigma-Aldrich). ELISA was performed according to the manufacturer's instructions to examine the levels of 12(S)-HETE, 15(S)-HETE (Assay Designs), human MCP-1, and mouse MCP-1 (Invitrogen).

Cell culture. Neonatal Wistar rats were purchased from Takasugi Experimental Animal Supply. Cardiomyocytes and cardiac fibroblasts were prepared from these neonatal rats and cultured as described previously (Sano et al., 2007). Human umbilical vein endothelial cells (BioWhittaker; Lonza) were cultured according to the manufacturer's instructions.

Luciferase assay. 1 μg of the reporter gene plasmid was transfected into COS7 cells at 24 h before the luciferase assay. 0.1 μg of the control vector encoding *Renilla* luciferase was cotransfected as an internal control. The assay was performed using a dual luciferase reporter assay system (Promega) according to the manufacturer's instructions. p55-A2-Luc (the luciferase reporter gene containing the κB binding site) was a gift from T. Fujita (The Tokyo Metropolitan Institute of Medical Science, Tokyo, Japan; Fujita et al., 1993).

Statistical analysis. Data are shown as the mean ± SEM. Multiple group comparison was performed by one-way ANOVA, followed by Bonferroni's test for comparison of means. Comparisons between two groups were done with the two-tailed unpaired Student's *t* test or two-way ANOVA. In all analyses, $P < 0.05$ was considered statistically significant.

Online supplemental material. Fig. S1 depicts *Alox15* transgenic animal data. Fig. S2 shows MCP-1 levels after treatment with 7ND. Fig. S3 shows a negative control of immunohistochemistry for 12/15-LOX. Fig. S4 shows blood pressure of *Alox15*-deficient mice. Table S1 summarizes the microarray data. Online supplemental material is available at http://www.jem.org/cgi/content/full/jem.20082596/DC1.

We thank Dr. C. Funk, Dr. T. Yoshimoto, and Dr. T. Fujita for reagents and E. Fujita, R. Kobayashi, Y. Ishiyama, and M. Ikeda for technical support.

This work was supported by a Grant-in-Aid for Scientific Research from the Ministry of Education, Science, Sports, and Culture, and Health and Labor Sciences Research Grants (to I. Komuro), a Grant-in-Aid for Scientific Research from the Ministry of Education, Culture, Sports, Science and Technology of Japan, grants from the Suzuken Memorial Foundation, the Japan Diabetes Foundation, the Ichiro Kanehara Foundation, the Tokyo Biochemical Research Foundation, and the Cell Science Research Foundation (to T. Minamino), grants from the Takeda Science Foundation and the Japan Foundation of Applied Enzymology (to T. Minamino and H. Toko), and Sakakibara Memorial research Grant from the Japan Research Promotion Society for Cardiovascular Disease (to H. Toko).

The authors declare no competing financial interests.

Submitted: 17 November 2008
Accepted: 29 May 2009

REFERENCES

Anand, I.S., R. Latini, V.G. Florea, M.A. Kuskowski, T. Rector, S. Masson, S. Signorini, P. Mocarelli, A. Hester, R. Glazer, and J.N. Cohn. 2005. C-reactive protein in heart failure: prognostic value and the effect of valsartan. *Circulation.* 112:1428–1434.

Andersson, C.K., H.E. Claesson, K. Rydell-Tormanen, S. Swedmark, A. Hallgren, and J.S. Erjefalt. 2008. Mice lacking 12/15-lipoxygenase have attenuated airway allergic inflammation and remodeling. *Am. J. Respir. Cell Mol. Biol.* 39:648–656.

Bernaudin, M., Y. Tang, M. Reilly, E. Petit, and F.R. Sharp. 2002. Brain genomic response following hypoxia and re-oxygenation in the neonatal rat. Identification of genes that might contribute to hypoxia-induced ischemic tolerance. *J. Biol. Chem.* 277:39728–39738.

Bleich, D., S. Chen, B. Zipser, D. Sun, C.D. Funk, and J.L. Nadler. 1999. Resistance to type 1 diabetes induction in 12-lipoxygenase knockout mice. *J. Clin. Invest.* 103:1431–1436.

Bolick, D.T., A.W. Orr, A. Whetzel, S. Srinivasan, M.E. Hatley, M.A. Schwartz, and C.C. Hedrick. 2005. 12/15-lipoxygenase regulates intercellular adhesion molecule-1 expression and monocyte adhesion to endothelium through activation of RhoA and nuclear factor-kappaB. *Arterioscler. Thromb. Vasc. Biol.* 25:2301–2307.

Bolick, D.T., S. Srinivasan, A. Whetzel, L.C. Fuller, and C.C. Hedrick. 2006. 12/15 lipoxygenase mediates monocyte adhesion to aortic endothelium in apolipoprotein E-deficient mice through activation of RhoA and NF-kappaB. *Arterioscler. Thromb. Vasc. Biol.* 26:1260–1266.

Braunwald, E. 2008. Biomarkers in heart failure. *N. Engl. J. Med.* 358:2148–2159.

Chen, X.S., U. Kurre, N.A. Jenkins, N.G. Copeland, and C.D. Funk. 1994. cDNA cloning, expression, mutagenesis of C-terminal isoleucine, genomic structure, and chromosomal localizations of murine 12-lipoxygenases. *J. Biol. Chem.* 269:13979–13987.

Cummins, E.P., and C.T. Taylor. 2005. Hypoxia-responsive transcription factors. *Pflugers Arch.* 450:363–371.

Cyrus, T., J.L. Witztum, D.J. Rader, R. Tangirala, S. Fazio, M.F. Linton, and C.D. Funk. 1999. Disruption of the 12/15-lipoxygenase gene diminishes atherosclerosis in apo E-deficient mice. *J. Clin. Invest.* 103:1597–1604.

Cyrus, T., D. Pratico, L. Zhao, J.L. Witztum, D.J. Rader, J. Rokach, G.A. FitzGerald, and C.D. Funk. 2001. Absence of 12/15-lipoxygenase expression decreases lipid peroxidation and atherogenesis in apolipoprotein e-deficient mice. *Circulation.* 103:2277–2282.

Dwarakanath, R.S., S. Sahar, L. Lanting, N. Wang, M.B. Stemerman, R. Natarajan, and M.A. Reddy. 2008. Viral vector-mediated

12/15-lipoxygenase overexpression in vascular smooth muscle cells enhances inflammatory gene expression and migration. *J. Vasc. Res.* 45:132–142.

Egashira, K. 2003. Molecular mechanisms mediating inflammation in vascular disease: special reference to monocyte chemoattractant protein-1. *Hypertension.* 41:834–841.

Fujita, T., G.P. Nolan, H.C. Liou, M.L. Scott, and D. Baltimore. 1993. The candidate proto-oncogene bcl-3 encodes a transcriptional coactivator that activates through NF-kappa B p50 homodimers. *Genes Dev.* 7:1354–1363.

Garg, R., and S. Yusuf. 1995. Overview of randomized trials of angiotensin-converting enzyme inhibitors on mortality and morbidity in patients with heart failure. Collaborative group on ACE inhibitor trials. *JAMA.* 273:1450–1456.

George, J., A. Afek, A. Shaish, H. Levkovitz, N. Bloom, T. Cyrus, L. Zhao, C.D. Funk, E. Sigal, and D. Harats. 2001. 12/15-Lipoxygenase gene disruption attenuates atherogenesis in LDL receptor-deficient mice. *Circulation.* 104:1646–1650.

Goldstein, S. 2002. Benefits of beta-blocker therapy for heart failure: weighing the evidence. *Arch. Intern. Med.* 162:641–648.

Hatley, M.E., S. Srinivasan, K.B. Reilly, D.T. Bolick, and C.C. Hedrick. 2003. Increased production of 12/15 lipoxygenase eicosanoids accelerates monocyte/endothelial interactions in diabetic db/db mice. *J. Biol. Chem.* 278:25369–25375.

Hayashidani, S., H. Tsutsui, T. Shiomi, M. Ikeuchi, H. Matsusaka, N. Suematsu, J. Wen, K. Egashira, and A. Takeshita. 2003. Anti-monocyte chemoattractant protein-1 gene therapy attenuates left ventricular remodeling and failure after experimental myocardial infarction. *Circulation.* 108:2134–2140.

Ishii, M., S. Hashimoto, S. Tsutsumi, Y. Wada, K. Matsushima, T. Kodama, and H. Aburatani. 2000. Direct comparison of GeneChip and SAGE on the quantitative accuracy in transcript profiling analysis. *Genomics.* 68:136–143.

Jin, G., K. Arai, Y. Murata, S. Wang, M.F. Stins, E.H. Lo, and K. van Leyen. 2008. Protecting against cerebrovascular injury: contributions of 12/15-lipoxygenase to edema formation after transient focal ischemia. *Stroke.* 39:2538–2543.

Kolattukudy, P.E., T. Quach, S. Bergese, S. Breckenridge, J. Hensley, R. Altschuld, G. Gordillo, S. Klenotic, C. Orosz, and J. Parker-Thornburg. 1998. Myocarditis induced by targeted expression of the MCP-1 gene in murine cardiac muscle. *Am. J. Pathol.* 152:101–111.

Kudo, I., and M. Murakami. 2002. Phospholipase A2 enzymes. *Prostaglandins Other Lipid Mediat.* 68-69:3–58.

Kuhn, H., and V.B. O'Donnell. 2006. Inflammation and immune regulation by 12/15-lipoxygenases. *Prog. Lipid Res.* 45:334–356.

Kuwahara, F., H. Kai, K. Tokuda, M. Takeya, A. Takeshita, K. Egashira, and T. Imaizumi. 2004. Hypertensive myocardial fibrosis and diastolic dysfunction: another model of inflammation? *Hypertension.* 43:739–745.

Lebeau, A., F. Terro, W. Rostene, and D. Pelaprat. 2004. Blockade of 12-lipoxygenase expression protects cortical neurons from apoptosis induced by beta-amyloid peptide. *Cell Death Differ.* 11:875–884.

Libby, P., and E. Braunwald. 2008. Braunwald's Heart Disease: a Textbook of Cardiovascular Medicine. Saunders/Elsevier, Philadelphia. 509 pp.

McDuffie, M., N.A. Maybee, S.R. Keller, B.K. Stevens, J.C. Garmey, M.A. Morris, E. Kropf, C. Rival, K. Ma, J.D. Carter, et al. 2008. Nonobese diabetic (NOD) mice congenic for a targeted deletion of 12/15-lipoxygenase are protected from autoimmune diabetes. *Diabetes.* 57:199–208.

McMurray, J.J. 1999. Major beta blocker mortality trials in chronic heart failure: a critical review. *Heart.* 82:IV14–IV22.

McNally, A.K., G.M. Chisolm III, D.W. Morel, and M.K. Cathcart. 1990. Activated human monocytes oxidize low-density lipoprotein by a lipoxygenase-dependent pathway. *J. Immunol.* 145:254–259.

Nagelin, M.H., S. Srinivasan, J. Lee, J.L. Nadler, and C.C. Hedrick. 2008. 12/15-Lipoxygenase activity increases the degradation of macrophage ATP-binding cassette transporter G1. *Arterioscler. Thromb. Vasc. Biol.* 28:1811–1819.

Natarajan, R., and J.L. Nadler. 2004. Lipid inflammatory mediators in diabetic vascular disease. *Arterioscler. Thromb. Vasc. Biol.* 24:1542–1548.

Ni, W., K. Egashira, S. Kitamoto, C. Kataoka, M. Koyanagi, S. Inoue, K. Imaizumi, C. Akiyama, K.I. Nishida, and A. Takeshita. 2001. New anti-monocyte chemoattractant protein-1 gene therapy attenuates atherosclerosis in apolipoprotein E-knockout mice. *Circulation.* 103:2096–2101.

Reilly, K.B., S. Srinivasan, M.E. Hatley, M.K. Patricia, J. Lannigan, D.T. Bolick, G. Vandenhoff, H. Pei, R. Natarajan, J.L. Nadler, and C.C. Hedrick. 2004. 12/15-Lipoxygenase activity mediates inflammatory monocyte/endothelial interactions and atherosclerosis in vivo. *J. Biol. Chem.* 279:9440–9450.

Sakashita, T., Y. Takahashi, T. Kinoshita, and T. Yoshimoto. 1999. Essential involvement of 12-lipoxygenase in regiospecific and stereospecific oxidation of low density lipoprotein by macrophages. *Eur. J. Biochem.* 265:825–831.

Sano, M., T. Minamino, H. Toko, H. Miyauchi, M. Orimo, Y. Qin, H. Akazawa, K. Tateno, Y. Kayama, M. Harada, et al. 2007. p53-induced inhibition of Hif-1 causes cardiac dysfunction during pressure overload. *Nature.* 446:444–448.

Seiler, A., M. Schneider, H. Forster, S. Roth, E.K. Wirth, C. Culmsee, N. Plesnila, E. Kremmer, O. Radmark, W. Wurst, et al. 2008. Glutathione peroxidase 4 senses and translates oxidative stress into 12/15-lipoxygenase dependent- and AIF-mediated cell death. *Cell Metab.* 8:237–248.

Wen, Y., J. Gu, S.K. Chakrabarti, K. Aylor, J. Marshall, Y. Takahashi, T. Yoshimoto, and J.L. Nadler. 2007. The role of 12/15-lipoxygenase in the expression of interleukin-6 and tumor necrosis factor-alpha in macrophages. *Endocrinology.* 148:1313–1322.

Wen, Y., J. Gu, G.E. Vandenhoff, X. Liu, and J.L. Nadler. 2008. Role of 12/15-lipoxygenase in the expression of MCP-1 in mouse macrophages. *Am. J. Physiol. Heart Circ. Physiol.* 294:H1933–H1938.

Yokoyama, C., F. Shinjo, T. Yoshimoto, S. Yamamoto, J.A. Oates, and A.R. Brash. 1986. Arachidonate 12-lipoxygenase purified from porcine leukocytes by immunoaffinity chromatography and its reactivity with hydroperoxyeicosatetraenoic acids. *J. Biol. Chem.* 261:16714–16721.

Zhu, D., M. Medhora, W.B. Campbell, N. Spitzbarth, J.E. Baker, and E.R. Jacobs. 2003a. Chronic hypoxia activates lung 15-lipoxygenase, which catalyzes production of 15-HETE and enhances constriction in neonatal rabbit pulmonary arteries. *Circ. Res.* 92:992–1000.

Zhu, H., Y. Takahashi, W. Xu, H. Kawajiri, T. Murakami, M. Yamamoto, S. Iseki, T. Iwasaki, H. Hattori, and T. Yoshimoto. 2003b. Low density lipoprotein receptor-related protein-mediated membrane translocation of 12/15-lipoxygenase is required for oxidation of low density lipoprotein by macrophages. *J. Biol. Chem.* 278:13350–13355.